

STUDY OF EROSION RESISTANCE OF ULCC BASED PRECAST WITH INDIGENOUS HIGH ALUMINA CEMENT

A

THESIS SUBMITTED IN PARTIAL FULFILLMENT
OF THE REQUIREMENT FOR THE DEGREE OF

Master of Technology
in
Ceramic Engineering

By
Niroj Kumar Sahu
Roll no: 207CR107



**Department of Ceramic Engineering
National Institute of Technology
Rourkela
2007 - 2009**

STUDY OF EROSION RESISTANCE OF ULCC BASED PRECAST WITH INDIGENOUS HIGH ALUMINA CEMENT

A

THESIS SUBMITTED IN PARTIAL FULFILLMENT
OF THE REQUIREMENT FOR THE DEGREE OF

Master of Technology
in
Ceramic Engineering

By
Niroj Kumar Sahu
Roll no: 207CR107

Under the guidance of
Prof. Japes Bera
&
Sk. Bashir Mohammed (OCL India Ltd. Rajgangpur)



**Department of Ceramic Engineering
National Institute of Technology
Rourkela
2007 - 2009**

CERTIFICATE

This is to certify that the thesis entitled, **“STUDY OF EROSION RESISTANCE OF ULCC BASED PRECAST WITH INDIGENOUS HIGH ALUMINA CEMENT”** submitted by **Mr. Niroj Kumar Sahu** in partial fulfillments of the requirements for the award of **Master of Technology** degree in **Ceramic Engineering** at **National Institute of Technology, Rourkela** is an authentic work carried out by him under our supervision and guidance.

To the best of our knowledge, the matter embodied in the thesis has not been submitted to any other University/ Institute for the award of any Degree or Diploma.

Supervisor
Prof. Japes Bera
Department of Ceramic Engineering
National Institute of Technology
Rourkela -769008

Supervisor
Sk. Bashir Mohammed
Ch. Manager Castable & Precast
OCL India Limited
Rajgangpur-770017

ROURKELA

Acknowledgement

It is with a feeling of great pleasure that I would like to express my most sincere heartfelt gratitude to **Prof. J. Bera**, Dept. of Ceramic Engineering, NIT, Rourkela for suggesting the topic for my thesis report and for his ready and noble guidance throughout the course of my preparing the report. I thank you Sir for your help, inspiration and blessings.

I would like to express my heartfelt thanks and deep sense of gratitude to my honorable research supervisor **Sk. Bashir Mohammed**, OCL India Limited, Rajgangpur for introducing me to this vast field of Monolithic Refractory, for his constant encouragement, efficient planning, constructive criticism and valuable guidance during the entire course of my work.

I express my sincere thanks to **Prof. S. Bhattacharyya**, Head of the Department of Ceramic Engineering, NIT, Rourkela for giving me the opportunity to go to OCL India Limited, Rajgangpur carrying my project and providing me the necessary facilities in the department.

I also express my thanks to **Dr.N.Sahoo**, Head of Technology group and **Mr.Biren Prasad**, Assistant General Manager, Concast Department, OCL India Limited, Rajgangpur for providing me the necessary facilities in the department. I would also wish to express my gratitude and sincere thanks to my honorable teachers **Prof. S. K. Pratihara, Dr. B. Nayak, Dr. S. K. Pal, Dr. R. Majumder** and **Mr. A. Choudhury** for their invaluable advice, constant help, encouragement, inspiration and blessings.

Submitting this thesis would not be possible without the constant help, encouragement, support and suggestions from Ph.D Scholars and friends of my Department. I am very much thankful to them for their time to help.

Last but not least I would like to express my gratitude to my parents and other family members, whose love and encouragement have supported me throughout my education. I would also express my sincere thanks to laboratory Members of Department of Ceramic Engineering, NIT, Rourkela and Research & Development Department, OCL India Limited, Rajgangpur for constant practical assistance and help whenever required.

NIROJ KUMAR SAHU

Abstract

Effect of indigenous cement on high temperature slag corrosion resistance of four different types of industrial ULCC composition has been investigated. Four type were as follows: (a) composition dominated by BFA aggregate, (b) composition dominated by WFA aggregate, (b) composition dominated by Densed Bauxite aggregate and (b) composition having Densed Bauxite fused alumina aggregate.

Two types of CA plus CA₂ based indigenous cements; (i) 70% Al₂O₃ containing and (ii) 80% Al₂O₃ containing, were investigated for the study. One established imported cement was also used to compare the properties of ULCC based on Indigenous cement. ULCC precast were prepared by industrial procedure such as; mixing of aggregates, cement and additives, granulometry, addition of water and casting, curing at room temperature and drying at 110°C. Physical, mechanical and thermo mechanical properties of ULCC were evaluated on as dried, 1000°C and 1450°C fired samples. Slag corrosion resistivity was tested in rotary drum by using 50:50 slag and metal.

It has been found that ULCC composition having higher amount of BFA aggregate shows better slag corrosion resistance when indigenous HAC are used. However ULCC containing WFA shows better slag resistance when 80% Al₂O₃ containing indigenous cement were used. It was found that slag resistivity mainly depend on fused alumina aggregate content of ULCC and compositions without having BFA and WFA shows very high (about 28%) erosion. It has been found that Fused Alumina aggregates are less prone slag erosion than Densed Bauxite. But with addition of WFA, the Slag erosion resistivity of Densed Bauxite based ULCC increases. 70% Al₂O₃ containing indigenous cement shows better erosion resistivity performance in presence of BFA. However 80% Al₂O₃ containing indigenous cement shows better performance in presence of WFA.

Contents

	Page No
Acknowledgement	ii
Abstract	iii
List of Figures	vii
List of Tables	ix
Abbreviations Used	x
Chapter 1: Introduction & Background	1-9
1.1. Introduction	
1.2. Background	
1.2.1 Classification of Castable	
1.2.2 Conventional castable and its Disadvantage	
1.2.3 Low Cement Castables and Ultra low Cement Castables	
1.2.4 Particle Packing, Dispersion and Rheology	
1.2.5 Aggregates and Additives	
1.2.6 Erosion mechanism	
1.2.7 Prevention of the erosion	
Chapter 2: Literature review	10-20
2.1 Particle size distribution	
2.2 Mixing and rheology	
2.3 Effect of curing time	
2.4 Hydration behaviour of CAC's	
2.5 Effect of additives	
2.6 Hydration of CACs with calcined alumina	
2.7 Hydration of CACs with Siliceous Material	
2.8 Dehydration kinetics of calcium aluminate cement hydrate	
2.9 Effect of Inorganic Salts/Alkali on Conversion-Prevention in HAC	
2.10 Reactivity of high-alumina cement	
2.11 High-performance concretes from CAC	
2.12 Flow, flow decay of alumina based castable	

- 2.13 Deflocculating mechanism
- 2.14 Dispersing effect of organic and inorganic deflocculants
- 2.15 Effect of aluminium addition
- 2.16 Effect of sintered and fused alumina
- 2.17 Behaviour of Andalusite
- 2.18 Mullitisation behaviour of calcined clay–alumina
- 2.19 Effect of mullite formation on properties of refractory
- 2.20 Objective

Chapter 3: Experimental Procedure

21-30

- 3.1 Materials and Compositions
- 3.2 Batch preparation
 - 3.2.1 Sieve Analysis of Castable mix
- 3.3 Sample Preparation
- 3.4 Evaluation of properties
 - 3.4.1 Normal Consistency of Cement
 - 3.4.2 Cement fineness test
 - 3.4.3 Setting time test
 - 3.4.4 CCS of Cement
 - 3.4.5 Determination of AP and BD of castable
 - 3.4.6 Cold Crushing Strength
 - 3.4.7 Cold Modulus of Rupture
 - 3.4.8 Permanent Linear Change on heating
 - 3.4.9 Hot Modulus of Rupture
 - 3.4.10 X-Ray Diffraction Analysis
- 3.5 Erosion Testing in Rotary Drum

Chapter 4: Results and Discussion

31-58

- 4.1 Chemical analysis of cement
- 4.2 X-ray diffraction study
- 4.3 Physical Properties of Cements
- 4.4 Characterization of Castable group-A
 - 4.4.1 Sieve Analysis of dry mix

- 4.4.2 Chemical Analysis of castable
- 4.4.3 Physical properties
- 4.4.4 Mechanical properties
- 4.5 Characterization of Castable group-B
 - 4.5.1 Sieve Analysis of dry mix
 - 4.5.2 Chemical Analysis of castable
 - 4.5.3 Physical properties
 - 4.5.4 Mechanical properties
- 4.6 Characterization of Castable group-C
 - 4.6.1 Sieve Analysis of dry mix
 - 4.6.2 Chemical Analysis of castable
 - 4.6.3 Physical properties
 - 4.6.4 Mechanical properties
- 4.7 Characterization of Castable group-D
 - 4.7.1 Sieve Analysis of dry mix
 - 4.7.2 Chemical Analysis
 - 4.7.3 Physical properties
 - 4.7.4 Mechanical properties
- 4.8 Comparison between the Erosion behaviors of different group of castables
 - 4.8.1 Castables with imported cement (CA-25)
 - 4.8.2 Castables with indigenous cements

Chapter 5: Conclusion

59-63

References

List of figures

- Fig.1.1 Refractory production in India
- Fig.1.2 Sector wise refractory consumption in India
- Fig.1.3 Phase diagram for the system $\text{CaO-Al}_2\text{O}_3\text{-SiO}_2$
- Fig. 1.4 Relation particle packing, dispersion technology and rheology
- Fig.2.1 Schematic particle size triangle
- Fig. 2.2 Schematic representation of temperature profile in arbitrary units (a.u.) as a function of time for a CAC suspension
- Fig. 3.1 Flow chart for preparation procedure of ULCC
- Fig. 4.1 XRD pattern of Imported Cement (CA-25)
- Fig. 4.2 XRD pattern of Imported Cement (HAC-70)
- Fig. 4.3 XRD pattern of Imported Cement (HAC-80)
- Fig. 4.4 Sieve Analysis of Castable group- A
- Fig. 4.5 Variation in A.P with temperature
- Fig. 4.6 Variation in B.D with temperature
- Fig. 4.7 Variation of CCS with temprature
- Fig. 4.8 Variation of CMOR with temprature
- Fig. 4.9 XRD pattern of the fired AS70 composition
- Fig. 4.10 Erosion behavior of Castable group-A
- Fig. 4.11 Photograph of eroded samples
- Fig. 4.12 Sieve Analysis of Castable group-B
- Fig. 4.13 Variation in AP with temprature
- Fig. 4.14 Variation in BD with temprature
- Fig. 4.15 Variation in CCS with temperature
- Fig. 4.16 Variation in CMOR with temprature
- Fig. 4.17 Erosion behaviour of Castable group-C
- Fig. 4.18 Photograph of eroded samples
- Fig. 4.19 Sieve Analysis of Castable group-C
- Fig. 4.20 Variation in A.P with temprature
- Fig. 4.21 Variation in B.D with temprature
- Fig. 4.22 Variation in CCS with temprature
- Fig. 4.23 Variation in CMOR with temprature

- Fig. 4.24 Erosion behaviour of Castable group-C
- Fig. 4.25 Photograph of eroded samples
- Fig. 4.26 Sieve Analysis Castable group-D
- Fig. 4.27 Variation in A.P with temprature
- Fig. 4.28 Variation in B.D with temprature
- Fig. 4.29 Variation in CCS with temprature
- Fig. 4.30 Variation in CMOR with temprature
- Fig. 4.31 Erosion behaviour of Castable group-D
- Fig. 4.32 Photograph of eroded samples
- Fig. 4.33 Erosion behaviour of different group of Castable with CA-25
- Fig. 4.34 Erosion behaviour of different group of Castable with HAC-70
- Fig. 4.35 Erosion behaviour of different group of Castable with HAC-80

List of tables

Table 1.1	ASTM Classification of Refractory Castable
Table 3.1	Chemical analysis (wt. %) of the raw materials
Table 3.2	Weight percent of raw materials used in different constables
Table 3.3	Sub grouping of Castable according to the type of cement
Table 4.1	Chemical Analysis (wt.%) of Cements
Table 4.2	Quantitative Phase present in different cements
Table 4.3	Physical Properties of different type of cements
Table 4.4	Chemical compositions of the Castable group-A
Table 4.5	Physical properties of Castable Group-A
Table 4.6	Mechanical properties of Castable group-A
Table 4.7	Semi quantitative analysis of 1450°C fired constables
Table 4.8	Chemical Compositions of the Castable group-B
Table 4.9	Physical Properties of Castable Group-B
Table 4.10	Mechanical Properties of Castable Group-B
Table 4.11	Chemical Compositions of the Castable group C
Table 4.12	Physical Properties Castable Group C
Table 4.13	Mechanical Properties of Castable-C
Table 4.14	Chemical Compositions of the Castable group-D
Table 4.15	Physical Properties of Castable Group D
Table 4.16	Mechanical Properties of Castable-D

Abbreviations Used

ASTM	America Standard for Testing and Materials
°C	degree Celsius
cm	centimeter
Kg	Kilogram
gm	gram
min	minute
C	lime (CaO)
A	Alumina (Al ₂ O ₃)
S	Silica (SiO ₂)
CAS ₂	Anorthite
C ₂ AS	Gehlenite
CA	Monocalcium aluminate
CA ₂	Calcium di-aluminate (Grossite)
C ₁₂ A ₇	Dodeca-calcium hepta aluminate (Maynite)
CA ₆	Calcium hepta aluminate (Hibonite)
AH ₃	Gibbsite
HAC	High Alumina Cement
AP	Apparent Porosity
BD	Bulk Density
CCS	Cold Crushing Strength
CMOR	Cold Modulus of Rupture
HMOR	Hot Modulus of Rupture
PLC	Permanent Linear Change
Wt%	Weight percent
μ or μm	micrometer

Chapter-1

Introduction and Background

1.1 Introduction

Refractories, a nonmetallic material, are hard to melt at high temperature with enough mechanical strength and heat resistance to withstand rapid temperature changes, including repeated heating and cooling. They have also good corrosion and erosion resistance to molten metal, glass, slag, and hot gases etc. Because of good thermal stability of refractories they are used in kilns, furnaces, boilers, incinerator and other applications in industries like iron and steel, non ferrous metals, cement, glass, ceramics, chemicals etc.

Total refractory production in India is projected about 1500,000 metric tons per annum on the basis of data represented in Fig.1.1 [1]. Approximately 70% of refractories manufactured are used in steel making industries, 12% used in cement industries, 4% in glass manufacturing and remaining in non ferrous and ceramic industries (Fig.1.2). Among different types of shaped and unshaped refractory production during 2004-05 in India, high Alumina constitute 35%, fire clay about 25%, basic refractories 19%, silica based refractories about 4%, monolithic about 15%, and special products constitute 2% [2].

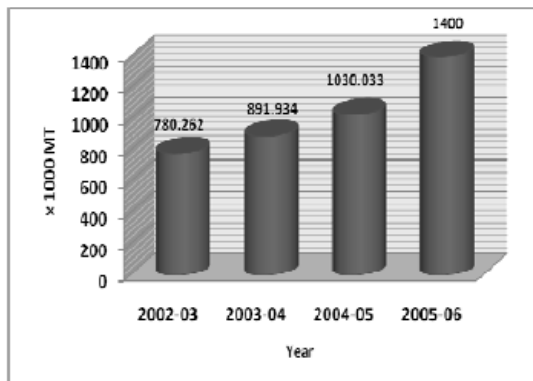


Fig.1.1 Refractory production in India.

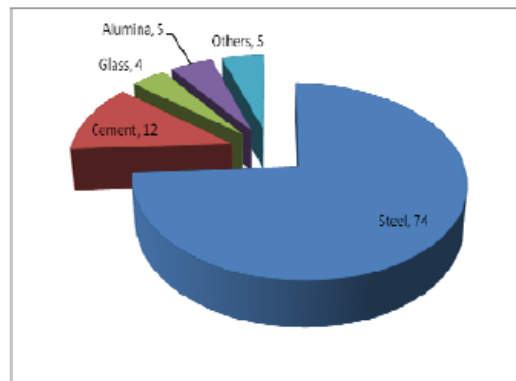


Fig.1.2 Sector wise refractory consumption in India [2].

Being a major consumer of refractory, steel industries control the demand and supply market of the refractory. As the production of crude steel increased, so the production of refractory also increased significantly. Besides, there has been a drastic change in the refractory technology in recent years. Strong demands are emphasized in various fields; like extended service life of the blast furnaces, rationalization, improvement of working environment,

energy saving and production of material with higher quality etc. The market conditions in the foundry and aluminum sector are similar to those seen in the steel industry. As a result of these trends the demand for refractory materials are high.

China continued to be the world's largest steel producer, accounting for more than 25% of total world production, and other emerging steel makers, including India, Russia, Ukraine and Brazil, remained strong. Presently India is producing around 32-34 Million tons steel per annum. Since India wants to get a fair share of the steel business, it has been already planned to produce 50-60 million tons of steel by 2011-12 and 100-120 million tons by 2020[3]. So keeping pace with the steel sectors, refractory sector is also growing rapidly. The most significant trend in refractories technology in the last two decades has been the ever-increasing use of monolithics, or unshaped refractories which now in many countries accounts for more than 50% of total production. Due to improved refractories quality their consumption has decreased dramatically in the last two decades while the ratio of monolithics to shaped refractories (bricks) has been steadily increasing [4-6]. Refractories still have many areas in various sectors to enter in and it would be the monolithics & special products that would dominate the production in future.

Monolithic refractory is the name generally given to all unshaped refractory products. They differ from the refractory bricks in that they are not shaped and fired before use, although the physical and technical properties exhibit similar and sometimes better characteristics. The reasons for the rapid growth of monolithics, at the expense of bricks are their ready availability, faster, easier and cheaper installation, fewer corrosion susceptible lining joints and similar performance as shaped product [6-10].

Monolithic refractories have a myriad of industrial applications throughout the steel, cement, non-ferrous metallurgical, waste disposal and petrochemical industries. They are available in many forms and different formulations. The main properties of these materials are their respective chemical inertness, mechanical integrity, abrasion resistance and thermal shock resistance at high temperatures. Monolithic consist of a wide variety of material types and compositions, with various bonding systems ranging from fluid cement pastes to stiff plastic lumps. The success of monolithics is due to significant advances in the type and quality of their binders, aggregates, and additives as well as to innovation in their design and installation techniques [7].

A significant advance in monolithics technology was the development of refractory concretes or castables based on calcium aluminate cements (CAC's) [7, 8]. Castables are complex refractory formulations, requiring high-quality precision-sized aggregates, modifying fillers, binders, and additives [11]. The majority of castables contain a CAC binder, although a few still use Portland cement [7]. The conventional castables, which contain the largest amount of cement, still make up the greatest percentage of those produced. The use of reduced cement varieties, low cement castables (LCC's) and ultralow cement castables (ULCC's), has grown significantly over the past 10 years [7]. This is because the CaO present in the cement leads to deterioration of high-temperature properties. They may be cast in moulds to form specific products (pre-cast shapes) or cast "in place", as when forming a lining for a kiln furnace. The main technical advantages of LCC's and ULCC's are their excellent physical properties, such as high density, low porosity, high cold and hot strengths, and high abrasion and corrosion resistance.

Many attempts are made to improve the thermo mechanical properties of refractory castable by reducing the cement content and using proper qualities of aggregates and matrix components as well as the quality of cement [8,9,12]. This thesis is related to ULCC. Hence a brief background about the same is very much essential to define the problem, understand its properties and ultimate application. Following section provides a brief background of the same.

1.2 Background

1.2.1 Classification of Castable

According to ASTM C401-91, Standard Classification of Alumina and Alumina Silicate Castable Refractories, the following classification exists regarding chemistry and lime content [12,13]. A proper classification should include as much information as possible about the chemical nature, rheological behaviour, and installation characteristics of the castable.

Table 1.1- ASTM Classification of Refractory Castable

CASTABLE CLASSIFICATION	LIME CONTENT
Regular Castable Refractory	CaO > 2.5%
Low Cement Castable Refractory	1.0% < CaO < 2.5%
Ultra Low Cement Castable Refractory	0.2% < CaO < 1.0%
No Cement Castable Refractory	CaO < 0.2%

1.2.2 Conventional castable and its Disadvantage

Conventional castables consist of graded refractory aggregates bonded with the aluminous hydraulic cements. The properties of these concretes depend largely on the choice of refractory aggregate and hydraulic cement [16]. They contain approximately 15-30% CAC. This amount of cement is necessary to achieve satisfactory strength at low and intermediate temperatures although it makes the material thirsty. The 8-15% water generally added during processing is mainly used to develop the hydraulic cement bond (6-10%) and to make the concrete flow (2-6%), allowing its proper installation. However, a relatively large amount of water (0-5%) is often taken up by the porosity of the aggregates and does not contribute to the hydraulic bond.

These high-cement castables have three major disadvantages [11, 16].

1. They need so much water. So they are usually porous and open textured, which greatly reduces the strength. Although some of this porosity is due to entrapped air bubbles, most of it is caused by the excess water added on mixing. On heating, the hydraulic bond is first modified, as conversion takes place, and then destroyed by the dehydration process. During this textural modification, the pore size distribution changes and porosity grows significantly. The new porosity depends on the amount of chemically bonded water and is therefore dependent on cement type and content. The final open porosity of conventional refractory concretes fired at 1000°C generally varies from 22% to 26%, depending on the type of aggregate used.
2. Conventional castables show a characteristic drop in strength at intermediate temperatures (often quoted between 538°C and 982°C[17]), when the hydraulic bond has already broken down, due to the dehydration process, but the still sluggish sintering has not yet allowed the development of a ceramic bond.
3. Finally, the high-lime content of these castables favours formation of a fluid vitreous phase at high temperature via the eutectic liquid in the CaO-Al₂O₃-SiO₂ (CAS) ternary system (Fig.1.3) which may encourage crystal formation (e.g. mullite or spinel) but often will remain as a glass or low melting anorthite and gehlenite on cooling which degrades refractoriness and corrosion resistance.

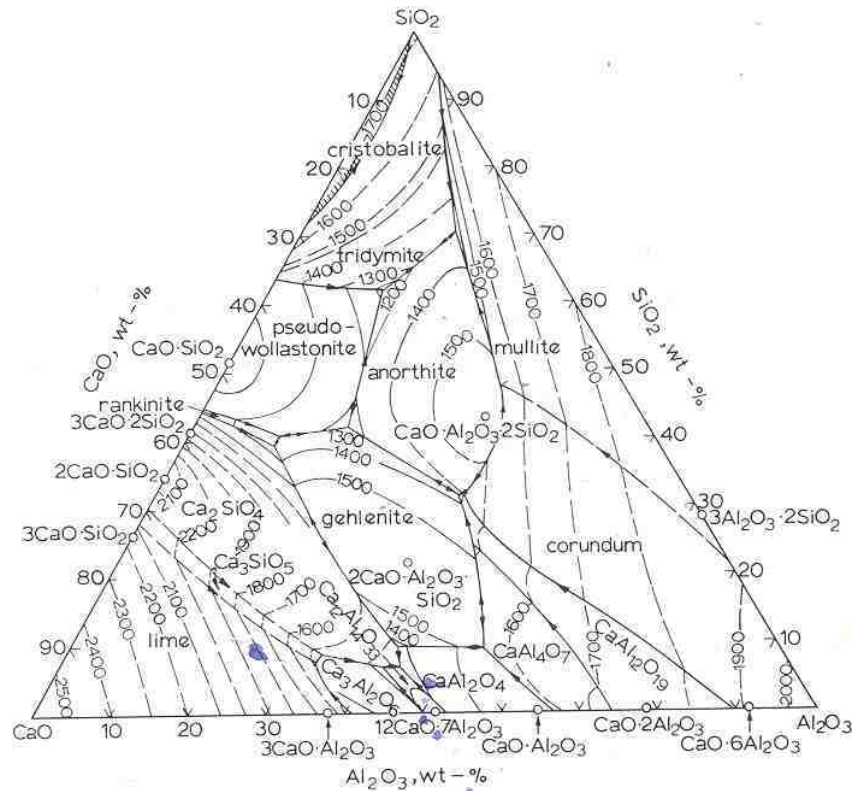


Fig. 1.3 - Phase diagram for the system $\text{CaO-Al}_2\text{O}_3\text{-SiO}_2$ based mainly on the work of Rakine & Wright[18].

Even with a high-purity CAC containing 70-80 wt% Al_2O_3 , it is impossible to reduce the CaO content of conventional castables to less than 3%, which is still a high amount, particularly if silica-containing aggregates are used. Further reduction is only possible by reducing the cement content. Reducing the amount of cement without spoiling other properties of the material proved difficult and challenging, but after several attempts it finally led to the development of a new range of products: the low and ultralow cement castables.

1.2.3 Low Cement Castables (LCC's) and Ultra low Cement Castables (ULCC's)

Refractory castables with no more than 5-8wt% cement, characterized by excellent cold and hot strengths, were first mentioned in a French patent granted in 1969 to Prost and Pauillac [6]. Reduction of the cement content without any reduction in strength was accomplished by the addition of approximately 2.5 to 4wt% fine ($< 50\mu\text{m}$, but ideally less than $1\mu\text{m}$) clay minerals and 0.01 to 0.30wt% deflocculants (such as alkali metal phosphates and carbonates). The objective was to reduce the amount of water by promoting a homogeneous distribution of

the cement so that the hydraulic bond could be fully utilized. Despite their lower porosity and better corrosion resistance, compared to conventional castables, the first generation of LCC's was too sensitive to rapid heating, mainly because the chemically bonded water was released in a much narrower temperature range[19] This led to explosive spalling since the outer layers closed off and internal water pressure built up. Further improvements led to the development of concretes characterized by a pseudozeolithic bond, which releases the chemically bonded water slowly between 150°C and 450°C, rather than within a narrow temperature range [19, 20]. This minimized the problems associated with explosions during heating, but, because LCC's and ULCC's are dense materials with low permeability, baking out is always difficult, especially in thick installations [13].

1.2.4 Particle Packing, Dispersion and Rheology

The main idea behind LCC's and ULCC's is to reduce the water requirement for placement while maintaining strength. A major breakthrough in the development of this technology is the inter-relation between particle packing, dispersion technology, and rheology of the castables. Understanding the relation between the first two of these gave rise to the new range of LCC's and ULCC's, while incorporating the third further improved the overall understanding of the technology and allowed the development of SFC's (Fig.1.4). More efficient particle packing reduces the maximum size of the interstices between particles. For a size distribution which packs more efficiently, less of the liquid is segregated in large interstices and more of it is effectively mobilized in flow. So for castable formulation, it is more important to have a clear understanding about the aggregates and additives.

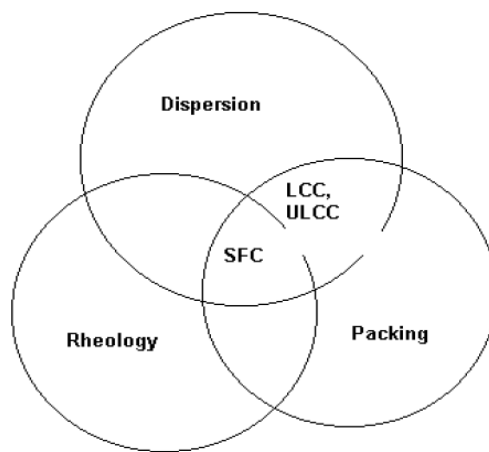


Fig. 1.4 - Relation particle packing, dispersion technology and rheology

1.2.5 Aggregates and Additives

LCC's and ULCC's are basically a mix of two main components: the refractory aggregate (particle fraction above 45 μ m) and the binding system (particle fraction below 45 μ m). The aggregate system normally comprises 60-85wt% of the castable mix, and its chemical composition and physical characteristics significantly affect the final properties of the castable, particularly thermal shock and corrosion resistance. Practically any natural or synthetic refractory oxide that is normally used for refractory bricks can be used as aggregate in LCC's and ULCC's. However, alumina, fused or sintered, is the most common aggregate used due to its high strength, relatively low thermal expansion coefficient, and good resistance to chemical attack.

The fine fraction below 45 μ m usually represents the bond system, which consists of the hydraulic binder, fine and superfine ceramic powders, and admixtures of deflocculants, water reducing agents, set retarders and accelerators. This fraction will become the matrix of the solid concrete after setting and will give rise to a ceramic bonding phase upon firing, which will bind together the initial particles of refractory aggregates. Due to its multiple roles in controlling the flow behaviour and setting time of the castable, as well as the strength and properties of the binding ceramic matrix, the selection of these materials is most important for LCC and ULCC.

The main role of the submicron powder additions is to act as filler, exactly filling the void spaces between the larger particles, so that the densest possible packing is achieved. Submicron powders commonly used are alumina, silica, chromium oxide, zirconia, titanium oxide, silicon carbide, clay minerals, and even carbon. Use of microsilica is claimed to reduce the open porosity from about 20-30% to 8-16% after firing at 1000°C, and that this reduces the characteristic drop in strength at intermediate temperatures often observed in conventional castables[21,22]. The material is highly reactive in cementitious and ceramic bond systems, leading to improved ceramic bonding (forming e.g. mullite and forsterite) at reduced firing temperatures both in high-alumina and magnesia-based products. Studies with microsilica-containing cement pastes have shown that microsilica reacts with the calcium aluminate phases in the cement and water to form zeolitic CASH phases. The zeolitic phases do not release their chemically-bonded water abruptly in a narrow temperature interval. This phenomenon increases the spalling resistivity of the castables.

Reactive alumina whose relatively high-surface area fine crystals exhibit higher densification and reaction rates when compacted and sintered into ceramic products. Sintering temperatures required to completely densify ceramics made from fine superground alumina are usually 200°C lower than those made from regular ground, coarser alumina. The use of fine reactive alumina results in LCC's with excellent hot properties and very low mixing water requirements for placement.

However, the idea of reducing the water requirement for placement by simply improving the packing density of the castable would not have been successful without the proper use of additives to allow adequate dispersion of the submicron powders. Deflocculants are used separately or in combination with each being used in small amount (0.05 - 0.5wt%) to deflocculate a particular type of particle. between 0.05 and 0.5wt%.

1.2.6 Erosion mechanism

Erosion of the refractory is defined as the deterioration of the refractories by the mechanism of corrosion and abrasion. Abrasion is the mechanism of wear out of refractory materials mechanically. It occurs at the interface of refractory lining by the friction of turbulent flow of molten metal and impingement of dust containing hot flues gases.

Corrosion of the refractories is defined as the deterioration of the refractories structure due to chemical reaction between the refractories materials and liquid metal, slag or gasses in contact with it followed by wearing or erosion. The corrosion of the refractories is the one of the main cause of refractories wear and tear during use [23]. Hence understanding of the actual mechanism involved in the corrosion will help in improving its performance. When liquid metal or slag come in contact with refractories surface the following sequence of event happens depending on the characteristics of both refractories and liquid/slugs in contact:

- a) Wetting
- b) Chemical reaction and generation of low melting liquids
- c) Penetration through pores
- d) Consequent wearing

The possibility of starting a chemical reaction between the refractory and the liquid in contact will be decided by their chemical compatibility, wettability, physical characteristics i.e. pore in the refractories and thermal state. The mechanism of corrosion is basically controlled by a

chemical process that changes to a diffusion controlled reaction which is temperature dependent. It is well established that higher temperature increase the corrosion rate. At higher temperature viscosity of slag reduces and wettability increase which helps in increasing the corrosion rate. Higher temperature increases the depth of penetration which in turn increases in wear rate.

1.2.7 Prevention of the erosion

Wear of refractories due to corrosion can be made minimize by

- Use of low porosity precast shapes and controlling the pore size distributions
- Use of castables with reduced wettability
- Controlling the temperature for reducing wettability (molten metal)
- Controlling the temperature for controlling chemical reaction.

As high alumina cements are a key component of these formulation, although they are only added in small amounts, an attempt has been made here in this thesis work to investigate the effect of some high alumina cement on the properties of ULCC.

Before chalking out the objective of this thesis, an extensive literature review has been made to reduce the number of trials and not to repeat the same work in this specification system. Following section provides a brief literature review for the same.

Chapter-2

Literature Reviews

2.1 Particle size distribution

Hamed Samadi[24] investigated the effect of particle size distribution on the properties of castables. He predicted that, even with having the same formulation, if the particle size distribution is different, the physical properties of the castable are changed. He followed the following particle size distribution triangle (Fig-2.1) to predict flowability and strength for castable formulation.

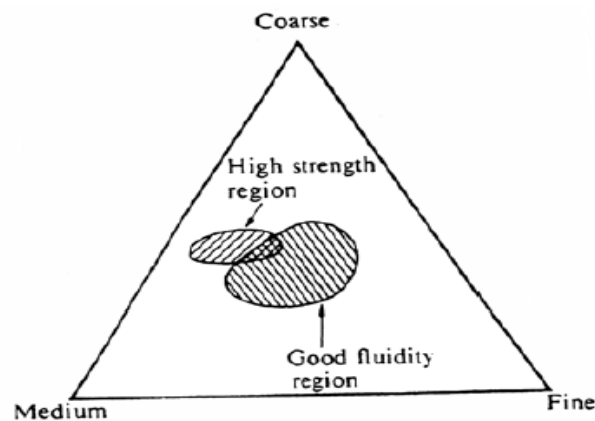


Fig 2.1 Schematic particle size triangle

He predicted that castables formulations with the particle size distribution in the intersection region between the high strength and good fluidity provides simultaneous good strength and better rheology. This region contains ~25% fines, ~20% medium and ~55% coarse particles.

2.2 Mixing and rheology

Rafael G. Pileggi et al. [25] investigated the influence of mixing on the rheological behavior of castables, evaluating the effects of particle size distribution, water addition rate and shear rate. They demonstrated that castables require a minimum mixing energy to reach maximum flow values, which was supplied by the two-step water addition method. This provides maximum mixing efficiency and greater castable fluidity. In contrast, although the torque values at the turning point using the one-step addition method were low, this procedure failed to display good efficiency in breaking up agglomerates. Coarse particle size distribution reduced the mixing time, but produced greater heating of the castables. Therefore, castables can be designed with particle

size distributions that result in high mixing efficiency combining low torque values at the turning point with short mixing times.

2.3 Effect of curing time

Fabio et al. [26] examined the influence of curing time on the properties of ultra-low cement high-alumina refractory castables cured at 10-50°C for the time period 2 hours to 30 days. They showed that mechanical strength and airflow permeability of the ULCC are associated with the diverse binding phases resulting from the hydration conditions and curing time. Samples cured at 10°C displayed very sharp decline in the permeability, reaching a significantly lower permeability level at the end of curing period and higher strength than the sample cured at 50°C. They observed that the association of low curing temperatures and high CA_2 compositions promoted long setting periods, causing a gradual drop in the permeability level and simultaneous gains in mechanical strength.

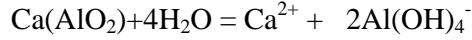
2.4 Hydration behaviour of CAC's

M. R. Nilforoushan et al. [27] have studied the role of different mineralogical phases present in the calcium aluminates cement on their hydration reactions and application properties in refractory castables. They showed that superior amounts of $C_{12}A_7$ in the cement shows flash setting behaviors in slurry with water cement ratio of 0.4. The cement with lower Blaine value affects the setting time of cement due to longer intrusion time required for penetration of water into the grains of cement. When the amounts of CA, CA_2 and $C_{12}A_7$ phases adjust by firing regimes, the cement will have reliable properties.

C. Alt et al. [28] studied the hydration profile of the calcium aluminate cement. They showed that during the hydration of the most reactive phases of calcium aluminate cement, heat is generated increasing the cement paste temperature and promoting the reaction even of the most inert phases. The hydration process occurs in three steps. A small temperature increase is observed when the hydration of calcium aluminate begins (region I, Fig.2.2), which is followed by a dormant period (region II). The hydrate precipitation is followed by an increase in the heat released (region III).

C.M.George et al.[29] shows that commercial calcium aluminate cements mainly consist of anhydrous phases: CA (40–70 wt%), CA_2 (<25 wt%) and $C_{12}A_7$ (<3 wt%). The CA_2 phase is the

most refractory and requires a long time to hydrate completely. Conversely, the $C_{12}A_7$ phase presents low refractoriness and needs a short time for hydration, and can speed up the setting time of the CA. As a consequence, the higher the $C_{12}A_7$ content in the cement, the faster the saturation and precipitation of hydrates is. This follows the following chemical equation:



The $Al(OH)_4^-$ ions formed impart a basic character to the suspension, as a small quantity of them dissociate into Al^{3+} and OH^- ions setting an equilibrium given by the basic constant K_b . As a result the pH increases. The reaction is

$$Al(OH)_4^- = Al^{3+} + 4OH^-, \quad K_b = \frac{[Al^{3+}][OH^-]^4}{[Al(OH)_4^-]} = 1.8 \times 10^{-2}$$

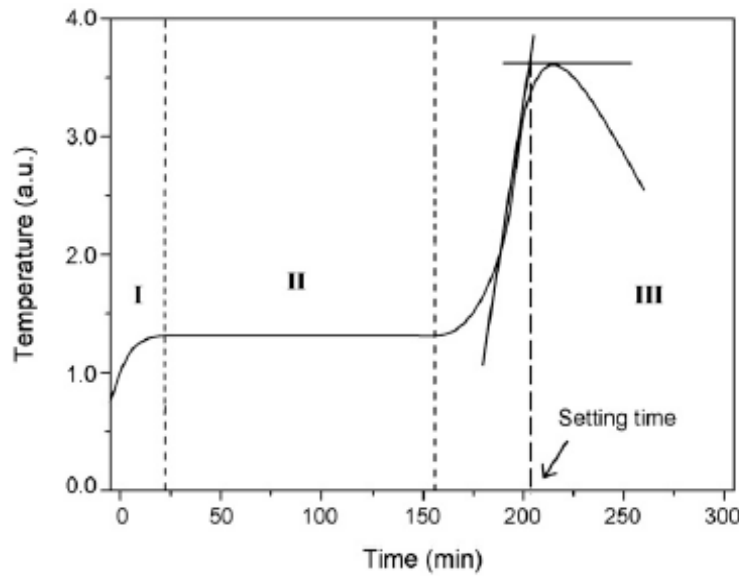


Figure 2.2 Schematic representation of temperature profile in arbitrary units (a.u.) as a function of time for a CAC suspension.

The dissolution of cement anhydrous phases increases the concentrations of the Ca^{2+} and $Al(OH)_4^-$ ions in solution up to the solubility limit, which is followed by the precipitation of a hydrated calcium aluminate phase. This allows further dissolution of the anhydrous phases and it is a cyclic process. The cement hydration kinetics decreases at lower temperatures, resulting in longer setting times.

J.M.Rivas Mercury et al. [30] studied the hydration behaviour C_3A , $C_{12}A_7$ and CA with added amorphous silica. The main hydrates found among the reaction products upon mixing water and amorphous silica with C_3A , $C_{12}A_7$ and CA at 40, 65 and 95 °C are katoite ($Ca_3Al_2(SiO_4)_{3-x}(OH)_{4x}$), gibbsite, AH_3 , amorphous phases like $Al(OH)_x$ and amorphous calcium silicate and calcium aluminosilicate hydrate phases (C–S–H and C–S–A–H). It has been shown that temperature plays an important role on the mechanism and formation rate of hydrated phases. In refractory castables most of the amorphous silica which does not enter the katoite host structure, acts as filler and increase the packing density. This improvement in the distribution of products results in an improvement of the structure of the castable, providing it more density.

2.5 Effect of additives

I.R. Oliveira et al. [31] have showed presence of matrix and additives (dispersants and accelerators) on the hydration process of hydraulic binders affect the setting and demolding time of shaped bodies. The dispersants presented a retarding effect on the hydration process, which is more significant for citric acid and diammonium citrate. The induction period is shortened by the presence of the matrix and addition of inorganic additives due to the formation of compounds such as $NaAl(OH)_4$ and $LiAl(OH)_4$, which withdraws $Al(OH)_4^-$ ions from the solution. It results in the increase of calcium ion concentration which induces the formation of less soluble hydrate and accelerates the precipitation stage. The combination of these additives with an accelerator (Li_2CO_3) was shown to be an efficient tool to control the setting time of castables.

S.A. Rodger et al. [32] have studied the effect of accelerators and retarders, in particular lithium salts and citric acid solutions, on the setting time of high alumina cement. They found that there is a nucleation barrier to the precipitation of the main products of hydration, CAH_{10} and C_2AH_8 . The lithium salts function as accelerators by precipitation of a lithium aluminate hydrate which acts as a heterogeneous nucleation substrate. They suggested that retardation by citric acid is due to the precipitation of protective gel coatings around the cement grains which impede hydrolysis or inhibit growth of the hydration products.

Thomas A. Bier et al. [33] showed Li_2CO_3 acts as the most effective accelerator for alumina cement. The hydration starts earlier and the set becomes smaller (steeper decrease in conductivity upon massive precipitation). They found the action of trisodium citrate as one of better retarder in calcium aluminate cement paste. It is observed that the prolonged setting time is due to much

slower dissolution of Ca^{2+} and $\text{Al}(\text{OH})_4^-$ ions with increasing citrate content. Also the precipitation of C_2AH_8 is even suppressed with high citrate concentrations. This entrains an improved workability.

N. Bunt et al. [34] studied the effect of additives on the calcium aluminate cement containing castables. They observed that chemical compounds delay the setting time by different mechanisms. The anions generated by these compounds in solutions are generally R-COO^- and R-O^- groups, which are strongly attracted by calcium ions. This characteristic has two consequences in the cement hydration process. Firstly, the reaction between these anions and Ca^{2+} generates insoluble salts in alkaline pH (pH of cement-containing media), decreasing the ratio between Ca^{2+} and $\text{Al}(\text{OH})_4^-$ ions in solution. As a result, the nucleation and growth of hydrates is slower, because the most soluble phase (AH_3) is favored. The second consequence is related to the precipitation of these insoluble salts on cement particles surface, resulting in a barrier on the solid-liquid interface that hinders further dissolution and delays the saturation stage.

2.6 Hydration of CACs with calcined alumina

I.R. Oliveira et al. [35] have shown that the induction period of cement hydration is shortened in the presence of matrix containing calcined alumina, which provide sites for the nucleation of cement hydrates and supplies Na^+ cations that most likely form the $\text{NaAl}(\text{OH})_4$ compound. This effect is enhanced by adding Li_2CO_3 , resulting in $\text{LiAl}(\text{OH})_4$. Thus, $\text{Al}(\text{OH})_4^-$ ions are withdrawn from the solution, increasing the $[\text{Ca}^{2+}]:[\text{Al}(\text{OH})_4^-]$ ratio, which favors the formation of less soluble hydrates, accelerating the precipitation stage. The additives, citric acid and diammonium citrate presented a significant retarding effect for the calcium aluminate binder.

2.7 Hydration of CACs with Siliceous Material

Benoit et al. [36] have studied the behavior of the cement in LCC and its interaction with fine fillers together with additives. They showed that hydration of calcium cement is modified in presence of microsilica. Fume silica, due to its role of retardation of the hydration of the CAC, facilitates the placement of low and ultralow cement castables. They observed that surface area and the soluble soda levels in fine alumina led to reduced flow and shorter working times as well

as an acceleration of the CAC hydration. They verified multiple additives system allows an optimization of the castable flow as well as flow decay. LCCs having only fume silica show a higher initial Young's modulus but those with alumina show an exponential increase in the young's modulus. The fluidity is governed by the electrostatic repulsion mechanism generated through particle-particle surface charges. These forces are modified by the dissolution of the CAC and normally provoke a flocculation which determines the end of fluidity and working time.

Tiwary et al. [37] have studied the hydrated phases formed by the interaction of the CACs and of siliceous material. They found that amorphous siliceous material is more reactive towards Calcium Aluminate Phases in CAC. Amorphous siliceous materials preferentially react with CA phase of CACs to yield a variety range of calcium aluminate silicate hydrate (CASH_x) phases. The hydrated phases mainly found are CAH_{10} , C_2AH_8 and AH_3 . Also the compositions of CASH_x strongly depend on the concentration of the CA and amorphous silica in the mix. The C/S ratio of CASH_x phase increases with increased CA concentration of the CAC Silica mix. At early stage of reaction, CASH_x phase of higher C/S ratio forms and with the progress of time, it further reacts with amorphous silica and yield CASH_x phase with lower C/ S ratio.

B.Myhre et al. [38] studied the influence of microsilica quality on properties of corundum-mullite self-flow ULCC. They showed that high-grade microsilica containing 98.3 % SiO_2 with alkali less than 0.6% and having a typical bimodal particle size distribution much better self-flow with excellent high temperature properties. The coexisting alkalies in low grade microsilica easily dissolve in water increasing its ionic strength. This could cause gelation and/or flocculation in the refractory castable and result in high viscosity and low self-flow. They showed that microsilica based castable possess higher HMOR and thermal shock resistance.

2.8 Dehydration kinetics of calcium aluminate cement hydrate

S. Maitra et al. [39] showed that calcium aluminate cement hydrate follows multistage dehydration with different reaction orders at different stages with different activation energies of dehydration. They described different dehydration stages with the rise in temperature in to the following phenomena:(i) Removal of surface bonded water (ii) Dehydration of aluminium hydroxide gel (iii)Dehydration of CAH_{10} to C_2AH_8 (iv) Dehydration of C_2AH_8 to C_3AH_6 (v) Dehydration of C_3AH_6 to anhydrous CA. The progressive collapsing of layers as a result of

dehydration probably increased the activation energy for dehydration at the initial stage, but afterwards the disintegration of the lattice at elevated temperatures caused a reduction in activation energy.

2.9 Effect of Inorganic Salts/Alkali on Conversion-Prevention in HAC

Jian Ding et al. [40] investigated the hydration characteristics and strength development of high alumina cement (HAC)/zeolite blended cement in combination with inorganic salts or alkalis. They found that HAC/zeolite mortars containing sodium salt (sodium sulfate, sodium carbonate, sodium nitrate, sodium metaphosphate, and sodium metasilicate) experienced no strength reduction after being water-cured at 38°C for 150 days. Stratlingite formation is apparently promoted and hydrogarnet formation is significantly inhibited by the addition of sodium salts.

2.10 Reactivity of high-alumina cement

Gaztafiaga et al. [41] studied the hydration reaction of high-alumina cement (HAC) at a temperature of 20°C and a water/cement ratio of 0.5 over a period of one month. During the hydration reaction of anhydrous cement a very complex and heterogeneous matrix develops which is formed by different solid hydrated as well as aqueous phase which plays an important role from the point of view of the durability of the hydrated material. They showed that cement hydration is a strongly exothermic reaction and strongly dependence on its surface area. The kinetic of hydration period follows in four steps: pre-induction (I), induction or latent (II), acceleration (III) and deceleration (IV) respectively. The main hydrated phases produced at 20°C (hexagonal (CAH_{10})) is metastable and over time tends to convert into the cubic one (C_3AH_6) more stable from a thermodynamic point of view. This change produces a decrease of the mechanical strength of the material.

2.11 High-performance concretes from CAC

Karen L. Scrivener et al. [42] studied corrosion and abrasion resistance in hydraulic structures of Calcium aluminates cements based concretes. They have observed that a calcium aluminate phase, on reaction with water formed hydrates is an exothermic process. They also showed that calcium aluminate cement hydrates shows better resistance to acid attack and possess good abrasion resistance. Control of the initial water-to-cement (w/c) ratio is very important to ensure

that the minimum strength is sufficient for the application. The conversion reaction in the hydrated phases leads to a continuously increasing development of strength.

2.12 Flow, flow decay of alumina based castable

Sankaranarayanan et al. [43] studied the effect of temperature, particle size distribution, additives and cement content on flow and flow decay of tabular alumina based self flow castable. They showed that the free-flow is influenced more by the microsilica, deflocculant, retarder and accelerator. The effect of accelerator or retarder means, the reduction of free flow due to excess additives (flocculating effect). They have showed that as the retarder content increase beyond certain limit the free flow is decreasing which can be compensated by the microsilica addition.

2.13 Deflocculating mechanism

Moreno.R et al.[44] studied role of additive on the rheological behavior of castable. Additives mainly include deflocculant, retarders and accelerators. They describe the mechanism of deflocculation in castable slurry. The inorganic deflocculant increase the zeta potential of colloidal particle and adds to repulsive force of static electricity between the particles, thus dispersing the particles. The organic deflocculant has a minor effect on zeta potential and its dispersing effect is believed to be mainly attributed to the steric stabilization. The stability of the suspension can be studied by means of the potential energy curves as a function of the separation between particles by DLVO theory.

2.14 Dispersing effect between organic and inorganic deflocculants

Z.Li, S.Zhang et al. [45] showed that retarder and accelerator primarily attack the $\text{Ca}^{2+}/\text{Al}(\text{OH})_4^-$ ratio of the system. Retarder influence the kinetics of hydration by modifying, usually slowing down the dissolution of the anhydrous cement particles. The mechanism involves reduction of dissolution by the absorption on the cement grain and/or combination with calcium ions. Retarder tend to decrease the $\text{Ca}^{2+}/\text{Al}(\text{OH})_4^-$ ratio by reacting with Ca^{2+} ions thereby diminishing the activity of them. Accelerators influence the period of hydration by forming germ thereby accelerating hydration. The accelerator reacts with $\text{Al}(\text{OH})_4^-$ thereby increasing the $\text{Ca}^{2+}/\text{Al}(\text{OH})_4^-$ ratio in solution. This promotes rapid hydrate formation, which result in accelerating of setting of setting time.

2.15 Effect of aluminium addition

Zhanmin Wang et al. [46] investigated influences of aluminum additions on properties of Al_2O_3 -SiC-C dry ramming mixes bonded by solid resin and with graphite as carbon source. They have shown that an optimum amount of aluminium additions served as sintering agent and anti-oxidant. In hydraulic based castables it assists to checks easy explosion and too long curing and drying time. It also contributes on the strength development of specimens treated at 1100°C and 1450°C by increasing bulk density and decreasing apparent porosity and linear shrinkage. Aluminium additions are contributive to hot MOR improvement. The use of Al (metal) powder helps the clay bonded castables[47] capable of quicker setting, rapid dry-out and improved strength. Its use checks explosive thermal spalling by increasing the permeability. Aluminum powder reacts with water at ambient temperature as follows:



The hydrogen gas formed escapes from the castables producing small channels. These channels then help steam leave the castable during the drying process.

Studart et al.[48] showed that the Al-H₂O reaction occurs in the castable much earlier and faster in the presence of calcium aluminate cement than in its absence. Due to its highly exothermic character, the Al-H₂O reaction occurs almost instantaneously releasing H₂ gas and forming new Al hydroxide species at the Al-H₂O interface. So presence of aluminum powder assists for faster and safer heating of castables.

2.16 Effect of sintered and fused alumina

Pavlo Kryvoruchko et al. [49] investigated the effect of sintered and fused alumina on the properties of alumina based refractory. They observed that sintered and white fused alumina are practically equivalent materials for production of alumina refractories with good properties of purity, open porosity, apparent density, cold crushing strength and refractoriness under load. However, the refractory of sintered alumina has higher thermal shock resistance, whereas refractory of white fused alumina has higher creep resistance. Both types of refractories have similar interaction with melted steel. However, the fused alumina has higher water absorption, open porosity and lower apparent density than the sintered alumina

2.17 Behaviour of Andalusite

P.Prigent et al. [50] studied the effect of fine andalusite particles in combination with various amounts of fume silica in the matrix of high alumina low cement castables. They have found that without andalusite, fume silica decreases the hot mechanical properties except if a high amount is added (8%). The addition of andalusite fines increases the refractoriness under load and the hot modulus of rupture at 1400°C, regardless of the fume silica content. Addition of andalusite fines is the most suitable solution to improve the hot mechanical properties of low cement castables in the system $\text{CaO-Al}_2\text{O}_3\text{-SiO}_2$.

2.18 Mullitisation behaviour of calcined clay–alumina

Viswabaskaran et al. [51] investigated the mullitisation behavior calcined clays different alumina sources such as reactive alumina, gibbsite and boehmite. The calcined clay (metakaolin) derived samples show better strength and density than the uncalcined clay derived sample. The bulk density is maximum for the mullite obtained from calcined clay and reactive alumina. The same trend was noted for all the clay and alumina sources. The kaolinite–metakaolin transformation proceeds very slowly, and metakaolin has an extreme defect structure results in lower density and flexural strength. The calcined clays also yield more perfect mullite crystals and hence better physical properties. The mullite formed from the calcined clays shows better physical properties. The mullite formation in the case of calcined clay with boehmite exhibits good mullite microstructure with high aspect ratio, due to purity, fine particle size and homogeneous mixing with clays. However the high water loss in boehmite creates surface cracks resulting in poor strength.

2.19 Effect of mullite formation on properties of refractory

M.F.M. Zawrah et al. [52] studied the effect of the mullite bond phase on the physico-mechanical and refractory properties of the refractory castables. They showed that ULCC containing only 2wt.% cement with 13 wt.% alumina/silica mixture and 85 wt.% well graded tabular alumina aggregate exhibited outstanding physico-mechanical and refractory properties after firing at 1500°C due to the presence of mullite in the bond phase with very little CaO. They found very trace amount of anorthite and prominent mullite phase formation in the ULCC fired at 1500°C. The formation of mullite as a bonding phase exhibits high refractoriness, low creep rate, low thermal expansion and thermal conductivity, good chemical and thermal stability and good

toughness and strength. This enables the use of ULCC in various refractory applications such as in steel, aluminium, copper, glass, cement, chemical and ceramic production.

H. Sarpoolaky et al. [53] studied the microstructural evolution on firing and quenching of a vibratable ultralow cement alumina castable made of aggregates(sintered, fused alumina) and hydratable alumina (HA), fumed silica and calcium aluminate cement(~1%) in the matrix.

They observed that CAS formation at 1200 °C resulted in increased pore size and a dramatic decrease in HMOR for Al-ULCC but they found superior high-temperature properties (HMOR) due to in situ mullite formation above 1400 °C.

2.20 Objectives

The main objective of this thesis work is to study the effect of indigenous cement (calcium aluminates cement) on the physical, mechanical and thermomechanical properties of the commercial ultralow cement based castables with following specific points:

1. To study the effect of indigenous high alumina cement having 70% Al_2O_3 content
2. To study the effect of indigenous high alumina cement having 80% Al_2O_3 content
3. To compare the properties of ULCC made of indigenous cement with that made of imported cement
4. To study the effect of high alumina aggregate variation
5. To study the effect of calcined clay aggregate addition

Chapter-3

Experimental Procedure

3.1 Materials and Compositions

Four commercial castable compositions under investigation were chosen for experiment. All the castables are vibratable ultralow cement alumina castable (ULCC). As the raw materials and their chemical compositions play an important role on the final refractories property of the castable, a brief study was done about the chemical composition of the individual raw material (Table-3.1) provided by the manufacturer before the castable formulation. The raw materials used for the preparation the castables are sintered alumina, white fused alumina(WFA), brown fused alumina(BFA),calcined clay, densed bauxite, microsilica, calcium aluminate cement(CAC), sodium hexa-metaphosphate (SHMP), aluminum powder and ammonium borate. The details chemical analysis of the raw materials was supplied by OCL INDIA Ltd, Rajgangpur.

Table 3.1 - Chemical analysis (wt. %) of the raw materials

Raw Materials	Al ₂ O ₃	SiO ₂	Fe ₂ O ₃	TiO ₂	Na ₂ O	K ₂ O	CaO	MgO	LOI
Calcined Clay	38	53	1.08	1.84	0.03	0.03	0.62		
Calcined Alumina	99.2	Trace	0.05				Trace		
WFA	99.64	Trace	0.04	Trace					
BFA	94.38	Trace	0.18	2.12			Trace		
Densed Bauxite	89.42	Trace	1.28	3.44					
Micro silica	0.4	97.89	0.10	Trace	0.10	0.20	0.15	0.30	1.01
Imported Cement	79.18	Trace	0.2				16.97		
Aluminum powder	Al metal=99.48								
SHMP					34.8		P ₂ O ₅ =65.2		

Four types of commercial castable compositions were chosen for investigation. The aggregate to matrix ratio was controlled to 65-70/35-30 (wt.%), with particle size distribution fitting for placement with vibration. The four type castables were grouped as Castable group-A, Castable group-B, Castable group-C and Castable group-D. Table-3.2 shows the weight proportion of different raw materials used for different castables. In each group of castable

three different type of cement are used individually keeping all others raw materials same. The weight percent of cement used was also made invariant. Accordingly in each group there are three subgroups. For example in Castable group-A, the subgroups are identified as A, AS70 and AS80 accordingly the imported cement (CA-25), indigenous cement-1(HAC-70) and indigenous cement-2(HAC-80) were used respectively and so for other groups. In this way twelve batches were prepared. Table-3.3 shows the classification of each group of castable according to the type of cement used. The indigenous cement are being manufactured by OCL INDIA Ltd, Rajgangpur.

Table 3.2 - Weight percent of raw materials used in different castables

Castable type	Castable Group-A	Castable Group-B	Castable Group-C	Castable Group-D
Calcined Clay	-	-	10	10
Calcined Alumina	10	5.0	7.5	-
WFA	15	57.5	5.0	
BFA	45	-	-	22
Densed Bauxite	25	32.5	71	62.5
Micro silica	3.0	4.0	4.0	4.0
C AC	2.0	2.0	2.0	2.0
Aluminium powder	0.5	0.4	0.5	0.4
SHMP	0.05	0.05	0.05	0.05
Ammonium Borate	0.02	0.02	0.02	0.02

Table 3.3 - Subgrouping of castable according to the type of cement.

Calcium Aluminate Cement	Batch			
	Group-A	Group -B	Group-C	Group-D
CA-25	A	B	C	D
HAC-70	AS70	BS70	CS70	DS70
HAC-80	AS80	BS80	CS80	DS80

3.2 Batch preparation

The batches were prepared by taking different grade of materials in proper proportion (Table-4.2). Each batch contains 20kg of materials. The materials were dry mixed in a pan mixer of 30kg capacity (rpm-32) for 25 minutes. After that 1kg material has been taken out for sieve analysis.

3.2.1. Sieve Analysis of Castable mix

1kg of dry mixed material was taken for testing. Then 200gm of material was separate out from it by Cone-Quartering method. The material was kept in a 1 litre container and then sufficient amount of water was added to form slurry. It was then transferred to the finest sieve of -325 mesh and washed by means of a small jet of water. Washed residue in the sieve was dried to constant mass at 110°C for 1hour. Then the dried residue was transferred to the sieve shaker consist sieve of different sieves of different meshes and vibration of frequency 50-60 Hz was given with an electromagnetic drive for 12 minutes. The weight of material remained in the different sieve was calculated as sieve percentage by weight. The following convention is used to characterize particle size by mesh designation:

- a "+" before the sieve mesh indicates the particles are retained by the sieve
- a "-" before the sieve mesh indicates the particles pass through the sieve

3.3 Sample Preparation

After dry mixing the castable mix wet mixing was performed as follows. Generally ultralow cement castables require less than 5 weight percent of water to achieve the desire rheology. As two step water addition is beneficial [25] our attempt of casting was as follows:

The casting was done by adding first two third proportion of water at a time. Then one third of water was added in a slow manner to get homogenous mixing. The wet mixing was performed up to 5-6 minutes to achieve proper flow. Flowability is represented by vibration flow value, measured using the flow cone with 100mm base diameter, 50mm high and 70 mm top diameter. The testing was performed on a vibration table working at 50 Hz of frequency and amplitude of 0.5mm. Immediately after wet mixing, the castable mix was

filled into the cone. The cone was placed in the vibrating table (according to ASTM norm Cone 240 C) filled with the castable. Then it was removed and the castable was subjected to 20 seconds of vibrations and allowed to spread. The resulting spread i.e. the ultimate diameter of the “cake” measured in millimeters was taken as the vibration flow value. Working time was determined to be the time after mixing at which the castable no longer flowed under vibration.

The homogenized mixture was cast into molds of 160x40x40mm onto a vibrating table with 50Hz vibrating rate. For each composition eight bar samples were prepared for laboratory testing. Two prismatic type samples were made for erosion testing (length 159.6mm, top base width 86mm, bottom base width 50mm, height 55mm). The detail of the sample preparation procedure is given the Fig.3.2. Then the samples were cured in a moisture saturated environment (95% Relative Humidity). After that the samples were demoulded and oven dried at 110°C for 24 hours. The test samples were fired at 1000°C and 1500°C in laboratory furnace with soaking time of 3hours.

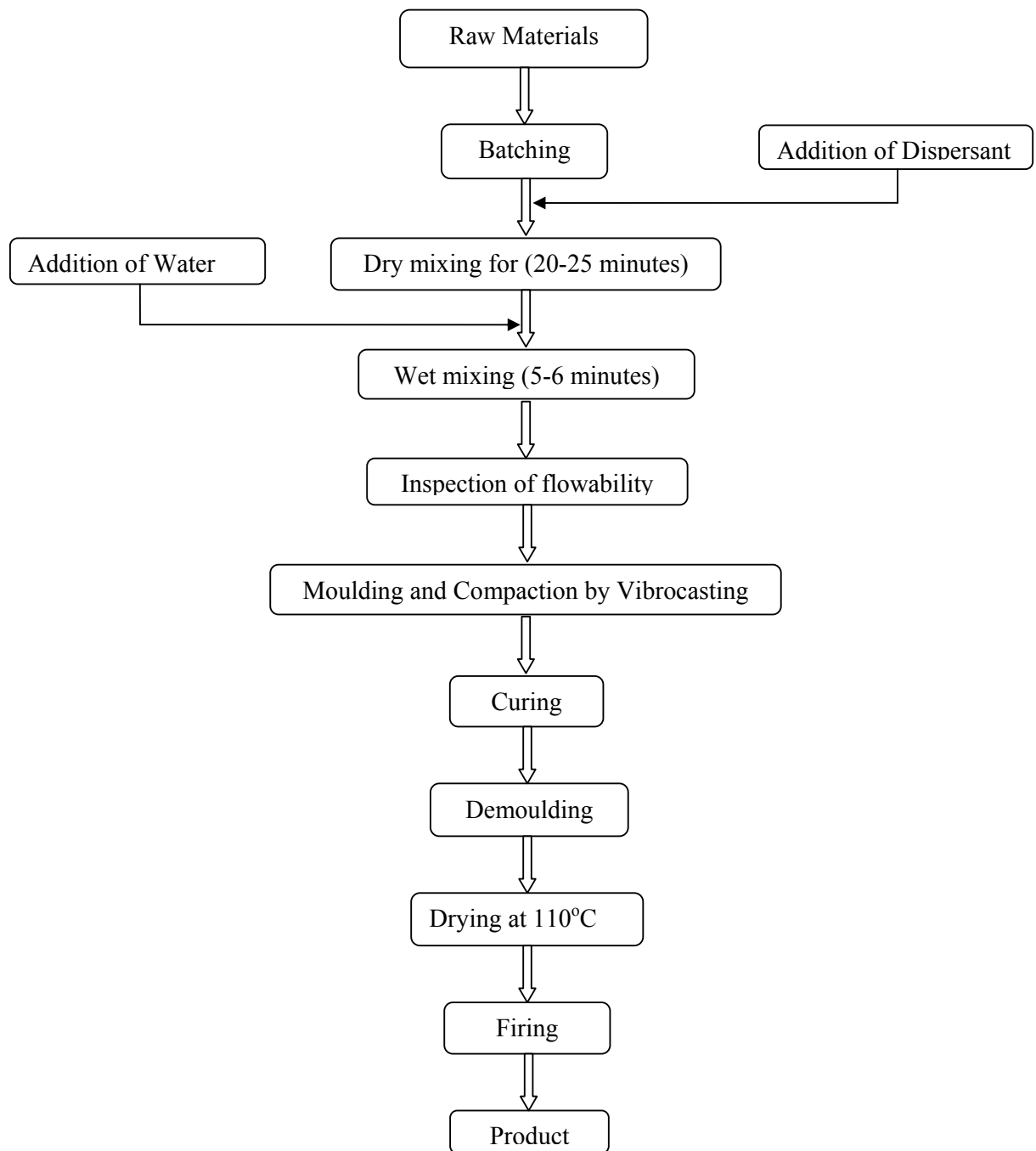


Fig. 3.2 - Flow chart for preparation procedure of ULCC sample

3.4 Evaluation of properties

As hydraulic binder is an important component of the castable formulation which generally provide the early strength to the castable and also decide the final refractory properties, the chemical and physical properties of the different type of cements has been evaluated. The chemical analysis of indigenous cements was done in the usual test procedure. The physical and mechanical properties namely bulk density (BD), apparent porosity (AP) and cold crushing strength (CCS), cold modulus of rupture (CMOR) of dried casted samples as well as samples fired at 1000°C and 1500°C have also been evaluated. After testing the CCS, the fractured samples were crushed, ground to -325 mesh sizes for chemical and X-ray diffraction study. The chemical analysis of the castable was supplied by the industry. The X-ray diffraction study of the cement has also been done. For the testing of above mentioned parameters the procedure adopted are as follows:

3.4.1 Normal Consistency of Cement

Normal Consistency is measure of plasticity of a cement paste. It refers to the degree of wetness exhibited by a freshly mixed concrete, mortar or neat cement grout whose workability is considered acceptable for the purpose at hand. It is measured as the amount of water was expressed as a wt.% of dry cement which permits the Vicat's plunger of 10mm diameter to penetrate to a point 5mm to 7 mm from the bottom of Vicat's mould with gauging time 3 to 5 minutes.

3.4.2 Cement fineness test

Fineness defines the surface area of cement particles present in per unit weight, which implies that more fineness means more particles in unit weight. This enhances the reaction rate which in turn will result in faster gain of strength at earlier stages. To test it 50 g sample of cement was placed on a clean and dry # 100 sieve (hole size of 0.15 mm), with the pan attached to it. sieving was done with a gentle wrist motion for about 9 minutes until most of the fine materials have passed through and the residue looks fairly clean. The amount of cement remained was weighed.

Calculation:

$$F = 100 - [(R_t / W)] * 100$$

Where F = fineness of cement expressed as the percentage passing # 100 sieve,

R_t = weight remaining in # 100 sieve, and

W = total weight of the sample in grams.

3.4.3 Setting time test

When water is mixed with cement, the paste so formed remains pliable and plastic for a short time. During this period it is possible to disturb the paste and remit it without any deleterious effects. As the reaction between water and cement continues, the paste loses its plasticity. This early period in the hardening of cement is referred to as 'setting' of cement. Initial setting time was measured by taking 500 g of cement and mixed with the percentage of water required for normal consistency. It is the time at which the concrete can no longer be properly mixed, finished or compacted (Represented by a Vicat needle penetration of 25 mm or less). So it represent the time when the cement paste loses its plasticity and stiffens considerably. Final setting time is the time required for the cement to harden to a point where it can sustain some load (Represented by no penetration of Vicat needle.)

3.4.4 CCS of Cement

Compressive strength (CCS) is the capacity of a material to withstand axially directed pushing forces. By definition, the compressive strength of a material is that value of uniaxial compressive strength reached when the material fails completely. CCS of cement was measured as the compressive strength of the cement mortars cube (7.07cm x 7.07cm x 7.07cm) made of 1:3 proportions with sand as fine aggregates, tested against compression.

3.4.5 Determination of AP and BD of the Castable

Apparent Porosity (A.P) is the ratio of the total volume of the open pores in a porous body to its bulk volume, expressed as a percentage, of the bulk volume. Porosity of refractory materials is a measure of percentage volume of pores with respect to bulk volume. Bulk Density (B.D) is the ratio of the mass of the dry material of a porous body to its bulk volume, expressed in g/cm^3 or in kg/m^3 . The bulk density is a measure of weight per unit volume and depends upon true specific gravity and the porosity.

The Archimedean method was used to measure A.P and B.D. To measure these properties, the test piece (65 × 65 × 40 mm) is dried at 110°C to constant mass, weighed in air, and then transferred to airtight vacuum chamber, which is then evacuated until a minimum pressure is reached. After the vacuum is maintained for a set time period, water is poured until the specimens are completely covered and to ensure open pores are filled. At atmospheric pressure, the specimens are reweighed while suspended in the liquid to determine the apparent mass, and then finally the soaked test piece is reweighed in air.

$$\text{Apparent porosity (\%)} = \frac{\text{Soaked Mass} - \text{Mass in air}}{\text{Soaked Mass} - \text{Suspended Mass}} \times 100$$

$$\text{Bulk Density} = \frac{\text{Mass in air}}{\text{Soaked Mass} - \text{Suspended Mass}} \times \text{Density of liquid (water)}$$

3.4.6 Cold Crushing Strength (CCS)

A mechanical compression testing machine is used to determine the cold crushing strength of the test specimen. 75mm cube test specimen was dried at 110°C and then cooled to room temperature. The load was applied on the sample in the flat position. The load was applied uniformly until the specimen failure.

$$\text{Cold Crushing Strength, in kgf/cm}^2 = W / A$$

Where W = Total maximum load in kgf, and

A = Average of the gross areas of top and bottom in cm².

3.4.7 Cold Modulus of Rupture (CMOR)

CMOR is measured as the maximum stress that a rectangular test piece (160 x 40x 40mm bar) can withstand when it is bent in a three-point bending device. The specimen was kept horizontally in a support having two edges and then load was applied on the sample uniformly during the test at a rate of 1.25 kgf per minute. The load (W) at the specimen failure was noted and modulus of rupture of the specimen calculated from the relation:

$$\text{CMOR, in kgf/cm}^2 = 3WL/2bt^2 \text{ kgf/cm}^2$$

Where L is the distance between bearing edges (cm); b is the width of specimen (cm); t is the thickness of the specimen (cm).

3.4.8 Permanent Linear Change on heating (PLC)

This test is intended for determining the permanent change of refractory bricks or shapes when heated under prescribed conditions. The test specimen (160 × 40 × 40mm) is heated up to 1000°C and 1450 °C with 3 hours of soaking period. Then initial length and the final length has been measured by a slide caliper and the PLC was calculated y using the formula

$$\text{PLC (\%)} = \frac{\text{Initial length} - \text{final length}}{\text{Initial length}} \times 100$$

3.4.9 Hot Modulus of Rupture (HMOR)

The samples were heated at 1400 °C. After being maintained at this temperature it soaked for 3 hours. Test pieces (40 mm × 40 mm × 160 mm) were then loaded at a constant rate of increase of tensile stress until failure occurs. The modulus of rupture (σ_f) is the ratio of the bending moment at the point of failure (M_{\max}) to the moment of resistance W, and is calculated from the following equation which is derived from Hooke's Law for elastic materials:

$$\sigma_f = \frac{W}{M_{\max}} = \frac{3F_{\max} L}{2bh^2}$$

Where, F_{\max} = Maximum force exerted on the test piece; L = Distance between the points of support of the test piece; b = Breadth of the test piece; h = Height of the test piece. The result is expressed in kg/cm².

3.4.10 X-Ray Diffraction Analysis

For X-ray diffraction (XRD), the samples were crushed and ground to less than -200 mesh. Then it was packed in a sample holder specially designed for x-ray diffractometer. The packed sample was inserted in to the XRD machine. Then the machine was switched on by supplying power to it. The XRD patterns were recorded on a unit (Philips PAN Analytical, The Netherland Electronic Instruments) using Ni-filtered Cu-K α ($\lambda = 1.54056\text{\AA}$) radiation working at 25 mA and 35 kV. Measurements were done on sample rotating at 0.04° per minute in the interval 20-70 degree (2 θ). After that phase analysis and quantification of different phases present in the sample were examined. The obtained diffraction patterns were smoothened, fitted and analyzed using Philips X-pert high score software. The semi quantitative phase analysis was done by Phillips JCPDS software.

3.5 Erosion Testing in Rotary Drum

First the dimensions of the casted prismatic type of castable samples were measured by slide calipers. About 9 samples were lined inside the rotary drum by using mortar for setting purpose. Then after drying (in room temperature) the drum was fitted to the rotary drum machine. Prior to the start of testing, the apparatus was connected to gas cylinders and the pressure of gas was checked properly. The rotating speed of the rotary drum was maintained at 5 rotations per minute. Before the start of testing with slag and metal, the samples were preheated at 1000°C for 1 hour. Then about 250 gm. of metal (iron rod) was added through the orifice of the sample holder. After 30 minutes 250gm of slag (LF) was put inside the sample holder. Simultaneously the temperature was increased to 1650°C by increasing the gas pressure and fuel supply. The temperature was kept constant at 1650°C for 1 hour. The temperature of testing was observed by means of pyrometer. After 30 minutes of testing, the molten metal and slag was tapped out from the machine and fresh slag and metal again added to it for further testing. Similarly another tapping was done after 30 minutes. In this way six number of tapping was done. Then it was left for one day for cooling purpose. In the next day it was delined and the samples were cut into two pieces longitudinally. Then the dimensions of the samples were checked and erosion percentage was calculated.

Chapter-4

Results and Discussion

Erosion behavior commercial ultra low cement castables (ULCC) with indigenous cement were investigated. A brief study was performed about the chemical analysis of all the raw materials used in the ULCC. The physical and chemical properties of the cements were evaluated. The raw materials and castable samples were characterized by XRD for phase analysis and quantification of different phases present. Apparent porosity, bulk density, cold compressive strength, cold modulus of rupture, hot modulus of rupture and permanent linear change on reheating properties of ULCC were measured. The erosion behavior of the ULCC based on indigenous cement was compared with that based on imported cement. Erosion properties were correlated with the physical, chemical and mechanical properties of the castables. This chapter describe in details the results and discussion about the same stated above.

4.1 Chemical analysis of cement

Calcium aluminate cements are a group of interrelated cementitious materials, with alumina contents varying from about 38% to 85%, and which incorporate monocalcium aluminate (CA) as the major constituent. The lime contents in the commercially available cements are ~16 to 27 %. Table 4.1 summarizes the chemical analysis result of different cements. It has been found that the imported cement (CA-25) and the indigenous HAC-80 contain ~ 80% alumina and 17 to 18 % of lime. However, the indigenous HAC-70 contains ~ 70 % alumina and ~26 % of lime. A very trace amount of Fe_2O_3 was found in all type of cements.

The calcium aluminate cement containing cent percent CA phase, the alumina contain is ~70%. Table-4.1 shows that CA-25 and HAC-80 contain ~80% alumina. So it is expected that these cement may contain some free alumina.

Table 4.1 - Chemical Analysis (wt.%) of Cements

Type of Cement	CA-25	HAC-70	HAC-80
Al_2O_3	79.18	72.04	80.94
Fe_2O_3	0.20	0.44	0.20
CaO	16.97	26.37	18.15

4.2 X-ray diffraction study

The XRD pattern of CA-25 is shown in the Figure-4.1. It is observed that CA-25 contains phases CA, CA₂, C₁₂A₇ and free α -Al₂O₃ phase. This result indicates that free α -Al₂O₃ phase is present in the cement. For that reason excess alumina was found in chemicals analysis (Table-4.1). Fig. 4.1 also shows that the major cementing phase of the cement is CA. however minor amount of CA₂ and C₁₂A₇ phases were detected. These phases were semi quantitatively estimated using Phillips X-pert high score software. The result of semi quantitative phase analysis for the cement is shown in the Table-4.2. It was found that the cement content about 31% free alumina and 54% CA phase.

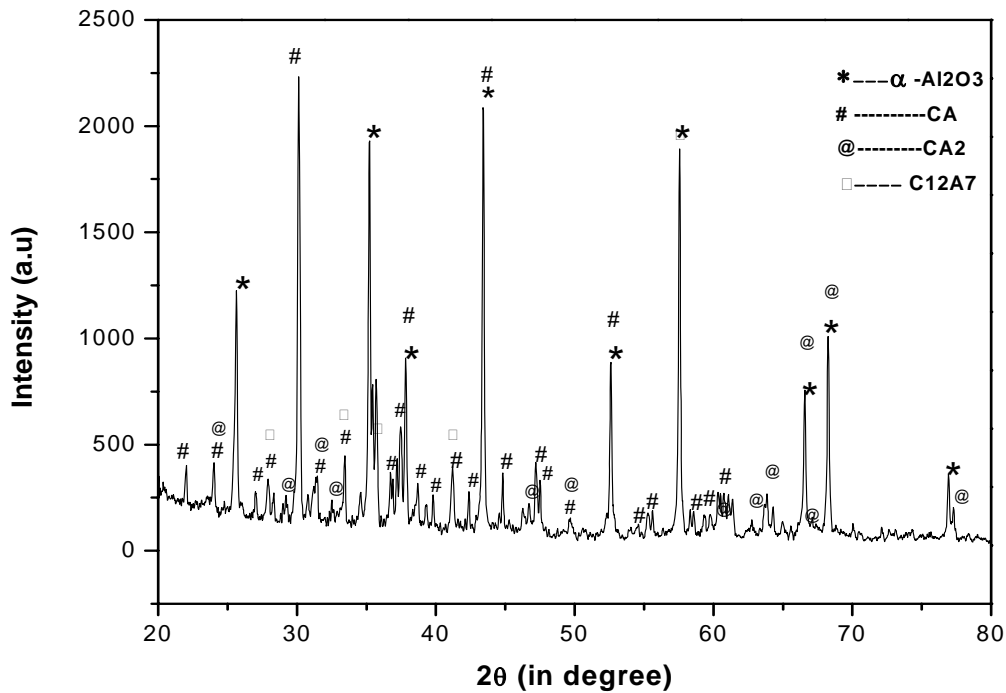


Fig. 4.1- XRD pattern of Imported Cement (CA-25)

Fig. 4.2 shows XRD pattern of HAC-70. It shows the presence of CA, CA₂, and C₁₂A₇ only. No corundum phases were detected. the phases were estimated semi quantitatively and the result is shown in Table 4.2. The result shows that the cement contains about 69% CA and 28% CA₂ only with minor amount of C₁₂A₇. So the major difference between imported cement and HAC-70 is the presence of CA₂ phase with higher concentration and absence of α -Al₂O₃.

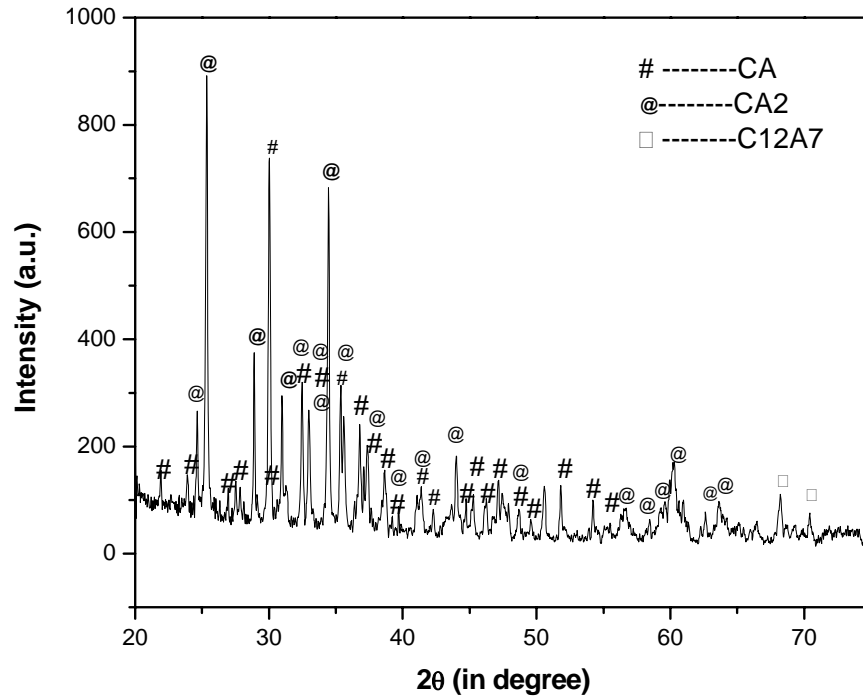


Fig.4.2 - XRD pattern of indigenous HAC-70

Fig. 4.3 shows The XRD pattern of HAC-80. As expected, there is the presence of free α - Al_2O_3 in the cement and its quantity (33%) is similar to that of imported cement CA-25. However, the major difference is the presence of CA_2 phase (19%) in the cement compared to the imported one.

The C_{12}A_7 phase in imported cement is much higher than the indigenous cements which may accelerate the setting of cement and affect the rheological behaviour of the castables containing HAC-70 [2]. The higher percentage of CA_2 in indigenous cements may accelerate the hydration behaviour of the CA phase providing relatively higher green strength to the castable as compared to the imported cement based castable [6]. Also this may increase the workability of the castable because of its slow rate of hydration.

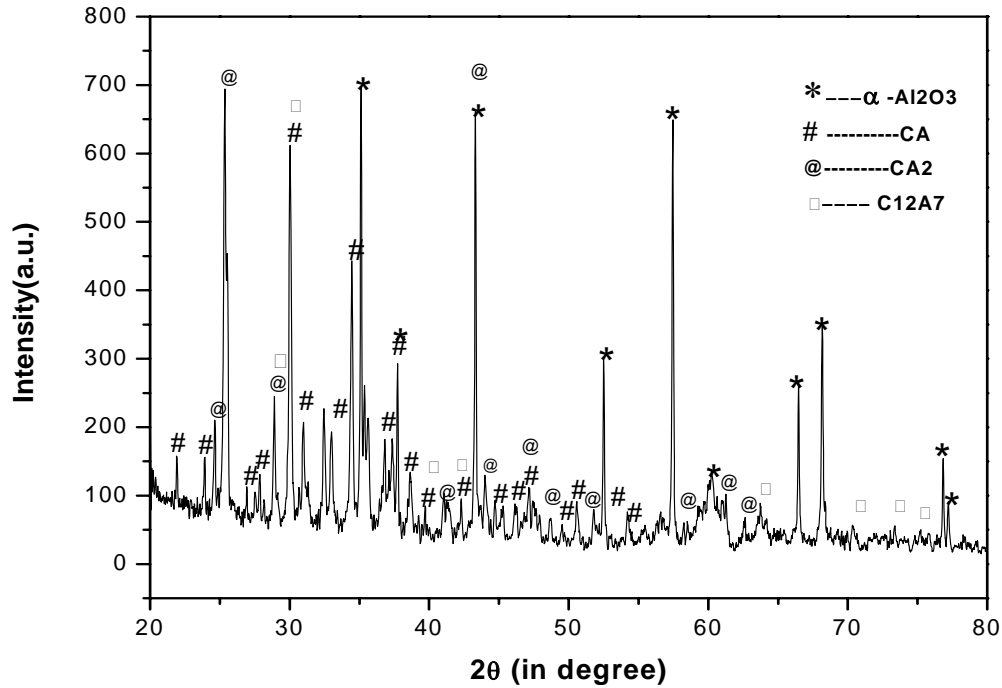


Fig.4.3- XRD pattern of indigenous HAC-80

Table 4.2 - Quantitative Phase present in different cements

Type of Cement	% of Different Phases			
	CA	CA ₂	C ₁₂ A ₇	Alpha- Al ₂ O ₃
CA-25	54	7	8	31
HAC-70	69	28	4	Trace
HAC-80	42	19	5	33

4.3 Physical Properties of Cements

Fineness of cement affects the water demand, hydration properties, workability and placeability of the concrete mixture. It is normally measured in terms of specific surface area. The average Blaine fineness of modern cement ranges from 3,000 to 5,000 cm²/g. Although cement with different particle distribution might have the same specific surface area, the specific surface area is still considered to be the most useful measure of cement fineness. Since hydration occurs at the surface of cement particles, finely ground cement will have a higher rate of hydration. Higher specific surface area means there is more area in contact

with water. The finer particles will also be more fully hydrated than coarser particles. However, the total heat of hydration at very late ages is not significantly affected. Table-4.3 shows that the surface area of imported cement is much higher than the indigenous cements. The higher fineness in the CA-25 is an indication of its higher surface energy. So its reactivity is more than the other two cements.

Table 4.3 - Physical Properties of different type of cements

Physical Properties	Type of Cement		
	CA-25	HAC-70	HAC-80
Cement fineness (cm^2/g)	7740	4480	4413
Normal Consistency (%)	34.0	27.8	37.0
Initial Setting time(min)	10	30	50
Final Setting time(min)	42	190	450
Green CCS (Kg/cm^2)	287	371	290
CCS/ 110°C (Kg/cm^2)	359	451	377

The normal consistency of the imported cement is ~ 35%. The normal consistency of HAC-80 is comparatively higher ~40% and HAC-70 is lower ~27%. The lower normal consistency of HAC-70 indicates that it needs lesser amount of water for the formation of pliable mass. The higher normal consistency of HAC-80 (37%) compared to HAC-70 may be due to the presence of free corundum powder in the cement. The normal consistency of imported cement is also high due to the same reason.

The initial and final setting times of the indigenous cements of the imported cement were comparatively lower than indigenous cements. This may be due to the very high fineness of imported cement. The initial setting times of the indigenous cements are more than the imported cement which imparts good workability. The final setting time of the imported cement is lesser than the indigenous cements and accordingly the demolding time is also less. The cold crushing strength of HAC-70 both in green and dried stage is comparatively better. The CCS of CA-25 and HAC-80 are found to be similar.

4.4 Characterization of Castable Group-A

4.4.1 Sieve Analysis of dry mix

The particle size distribution has an important role in the properties of refractory castable. Incorrect particle size distribution may cause dilatancy or the castable may need excess of water to be placeable. The particle size distribution of the fine fraction is generally determining the flow characteristics [24]. Fig.4.4 shows the sieve analysis of the castable group-A. The particle size having -0.06mm refers to the particles of size less than 45 μ m or -325 mesh. It has been observed that the fine fraction (diameter < 45 μ m) content in the different compositions is ~30%, the medium particle fraction (45 μ m < diameter < 1mm) ~20 % and coarse fraction (diameter >1mm) ~50 %. This particle size distribution is best suited in the overlapping region of good flowability and high strength [12].

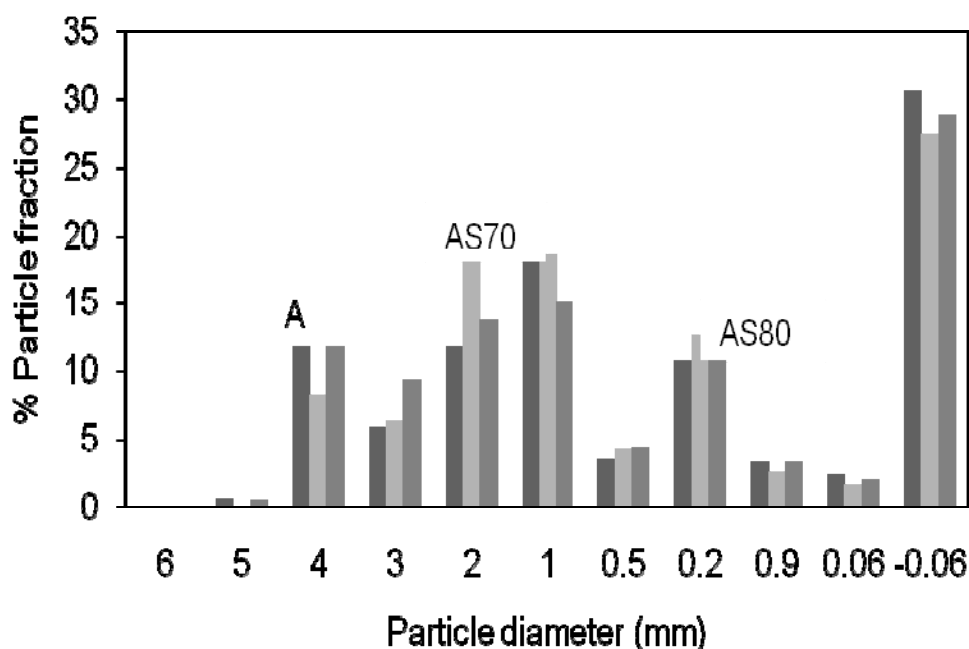


Fig. 4.4 Sieve Analysis of Castable group-A

4.4.2 Chemical Analysis of castable

The typical chemical analysis result of castables composition provided by the industry is shown in Table 4.4. In industrial practice only alumina, iron oxide, titanium oxide and lime has been tested for castable sample. The result shows that this group of castable contains more than 80% alumina. The higher percentage of alumina is due to use of higher percentage

of aluminous material (BFA~45%, WFA~15%, calcined alumina~10% and bauxite~25%). The lime contain in the indigenous cement HAC-70 is relatively higher due to higher lime content.

Table 4.4 - Chemical Compositions of the Castable group-A

Chemical Component (wt.%)	Castable group-A		
	A	AS70	AS80
Al ₂ O ₃	86.44	84.10	85.85
Fe ₂ O ₃	0.98	0.72	0.82
TiO ₂	1.72	1.82	1.78
CaO	0.60	1.11	0.80

4.4.3 Physical properties

The physical properties like water of casting, flow under vibration, initial setting time, apparent porosity, bulk density of castables are shown in Table-4.5. The water addition to a castable has a significant and direct influence on the final properties and castable specifications. Excess water can reduce strength and increase shrinkage, while too little water causes poor consolidation and placement which can produce voids in the castable.

The water demand for casting in AS70 is lesser than the other two compositions. This may be due to the lower normal consistency of the HAC-70 as compared to others because of its comparatively lower fineness. Water demand is measured industrially by visual examination of flowing characteristics of the slurry during the addition of water. Flowability of slurry primarily depends on dispersion and particle grading. HAC-70 cement may be responsible for better dispersibility of particles. All the compositions have more or less similar particle grading.

The setting times of all the compositions are in the working range. The setting time in AS70 is around 65 minute which is less than the setting time of AS80 (80 minute) and A (90 minute). This is because the water of casting in AS70 is less than the other two compositions. The flow in this composition is also found to be better than other two compositions. So the AS70 composition has a better rheology with a good workability. The setting time and flow

of the A and AS80 compositions are also in desire workable range. The good flow behaviors in all the compositions are due to well particle size distribution [24].

Table 4.5 - Physical Properties of Castable group-A

Physical Properties	Castable group-A		
	A	AS70	AS80
Water of casting (wt. %)	4.7	3.90	4.6
Vibro-flow(mm)	185	200	190
Initial Setting time(minute)	90'	65'	80'
Apparent Porosity 110°C/24hrs	11.1	7.6	11.3
1000°C/3hrs	14.3	9.9	14.5
1450°C/3hrs	14.6	8.8	13.9
Bulk Density(gm/cc)110°C/24hrs	3.09	3.24	3.09
1000°C/3hrs	3.06	3.21	3.05
1450°C/3hrs	3.10	3.22	3.09

The graphical representation of the variation of the apparent porosity and bulk density of different compositions with temperature are shown in Fig-4.5 and Fig-4.6 respectively. Generally the apparent porosity and the bulk density depend on the amount of casting water, dispersibility of the matrix and aggregate in the slurry and the packing of the structure. The apparent porosity and bulk density trend in 110°C dried specimens were found according to the water demand of casting. It is found that the apparent porosity in AS70 (7.6%) is less than the other two compositions A (11.1%) and AS80 (11.3%). This can be explained due to its good flow which provides better casting and packing in the mould. The bulk density was found in reverse order because the apparent porosity has an inverse relation with bulk density. The good bulk density i.e. above 3gm/cc in all the compositions is attributed to the use of higher percentage of fused alumina in the aggregate.

After firing at 1000°C, the apparent porosity of all the compositions increases on the basis of porosity at 100°C. This is due to the dehydration of the cementitious phases creating porous structure. It has been observed that the apparent porosity increases up to 1000°C then

decreases gradually with temperature. At around 1000°C the ceramic bond starts to form by sintering mechanism. The sintering mechanism is followed by dissolution-precipitation method at higher temperature resulting in the collapsing of pores and enhancing the densification mechanism. As the lime percentage in the cement used in AS70 is more, due to its fluxing nature it forms more liquid phases by reacting with fine alumina and silica leading to filling of pores and resulting in decreased of porosity and increased of bulk density at 1450°C.

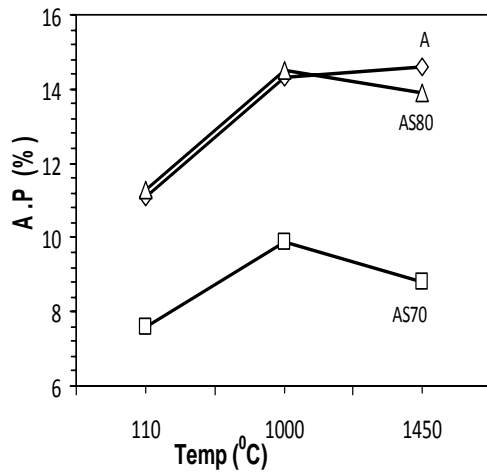


Fig. 4.5 Variation in A.P with temperature

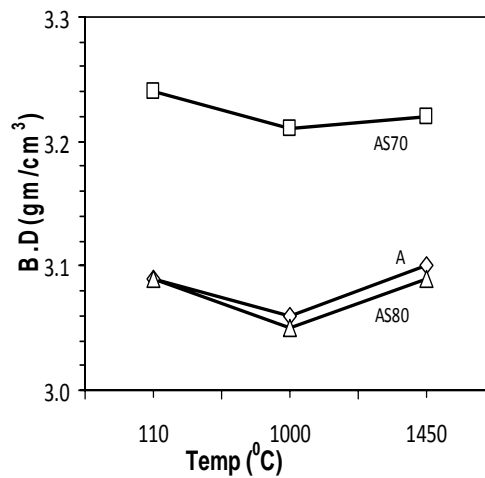


Fig. 4.6 Variation in B.D with temperature

4.4.4 Mechanical properties

The result of different mechanical and thermomechanical properties like cold crushing strength(CCS), cold modulus of rupture(CMOR), permanent linear change on heating(PLC), hot modulus of rupture(HMOR) and erosion characteristic of castable group-A is summarized in Table-4.6. The schematic diagrams of variation of CCS and CMOR with temperature are given in Fig-4.7 and Fig-4.8 respectively. Cold crushing strength of AS70 dried at 110°C is higher than others. This is because (1) higher B.D and low A.P of the specimen and (2) higher CA phases content around 69% in cement which provides a higher early strength to the castable in the green stage. In all type of sample the CCS trend observed to be increasing continuously with temperature. The increasing CCS at 1000°C is responsible to the formation of siloxane bond in the structure due to dehydration of C-A-S-H phase which provide a chain structure that binds the matrix and aggregate phases of the castable. At

1450°C the higher CCS is attributed to the formation of mullite which has a very good load bearing capacity.

Table 4.6 - Mechanical Properties of Castable group-A

Mechanical Properties	Castable group-A		
	A	AS70	AS80
CCS(kg/cm ²) 110 °C/24hrs	325	512	300
1000 °C/3hrs	606	668	594
1450 °C/3hrs	906	825	793
CMOR(kg/cm ²) 110 °C /3hrs	76	91	76
1000 °C/3hrs	167	122	160
1450 °C/3hrs	137	152	145
HMOR(kg/cm ²) 1400 °C/30min	16	22	13
PLC(%) 1000 °C/3hrs	+0.04	+0.06	-0.07
1450 °C/3hrs	-0.04	-0.09	+0.13
EROSION (%)	15.79	13.60	13.68

CMOR trend in all the compositions is found to be increasing upto 1000°C and than gradual decrease is observed. The higher temperature reduction can be attributed to the formation glassy phases which reduces the flexural strength of the castable due its brittle nature but CCS does not decreases rather increases. No sharp decrease in the CMOR in the high temperature is observed, because above 1350°C there is simultaneous formation mullite phase which provides both compressive and flexural strength of the castable compensating the brittle nature of the glassy phase formed. There is not so much impact of different type of cement on the CCS and CMOR has been observed at high temperature in this group of castable.

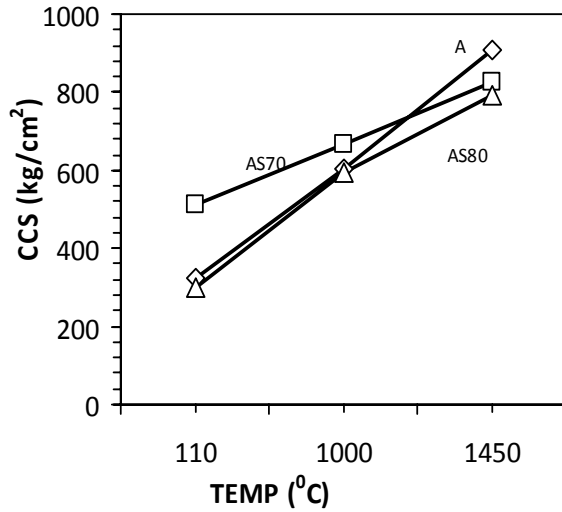


Fig. 4.7 Variation in CCS with temperature

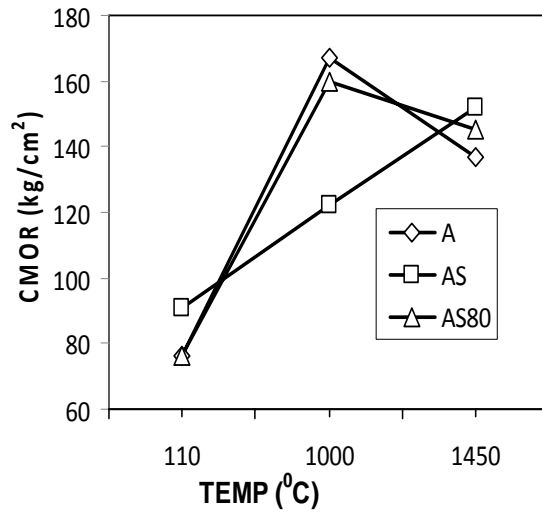


Fig.4.8 Variation in CMOR with temperature

The HMOR of AS70 is found superior than the other two compositions mainly due to highest BD and lowest AP that found at 1450°C (Table-5.6). These castables having higher amount of lime generally show the inferior high temperature behavior. This is because due to the fluxing [25] nature lime it forms higher amount of glassy phases like gehlenite and anorthite by reacting with fine silica and alumina deteriorating high temperature properties. From XRD analysis (Fig-4.9), it was found that in 1450°C fired AS70, alumina is the highest percent and also mullite is significant one (Table 4.7) which provides higher HMOR though small amount of glassy phase is present.

PLCs values for all the samples are negligible falling in the specification of ULCC. the slight positive and negative PLCs comes from volume expansion precipitation of mullite followed by and volume shrinkage followed by liquid phase formation.

The graphical representation of the erosion percentage of different compositions of Castable group- A as given in Table-4.7 is shown in Fig.4.10. The photo graph of the eroded sample after demolding from rotary drum is shown in Fig.4.11. The more resistance to the penetration of slag and molten metal in AS70 is because of its dense structure. Type A castable which is made by using imported cement shows less resistance to erosion and corroded more. This is because the corrosion and abrasion of the sample depends directly upon the porosity of the microstructure. This castable contains less amount of free alumina at 1450°C.

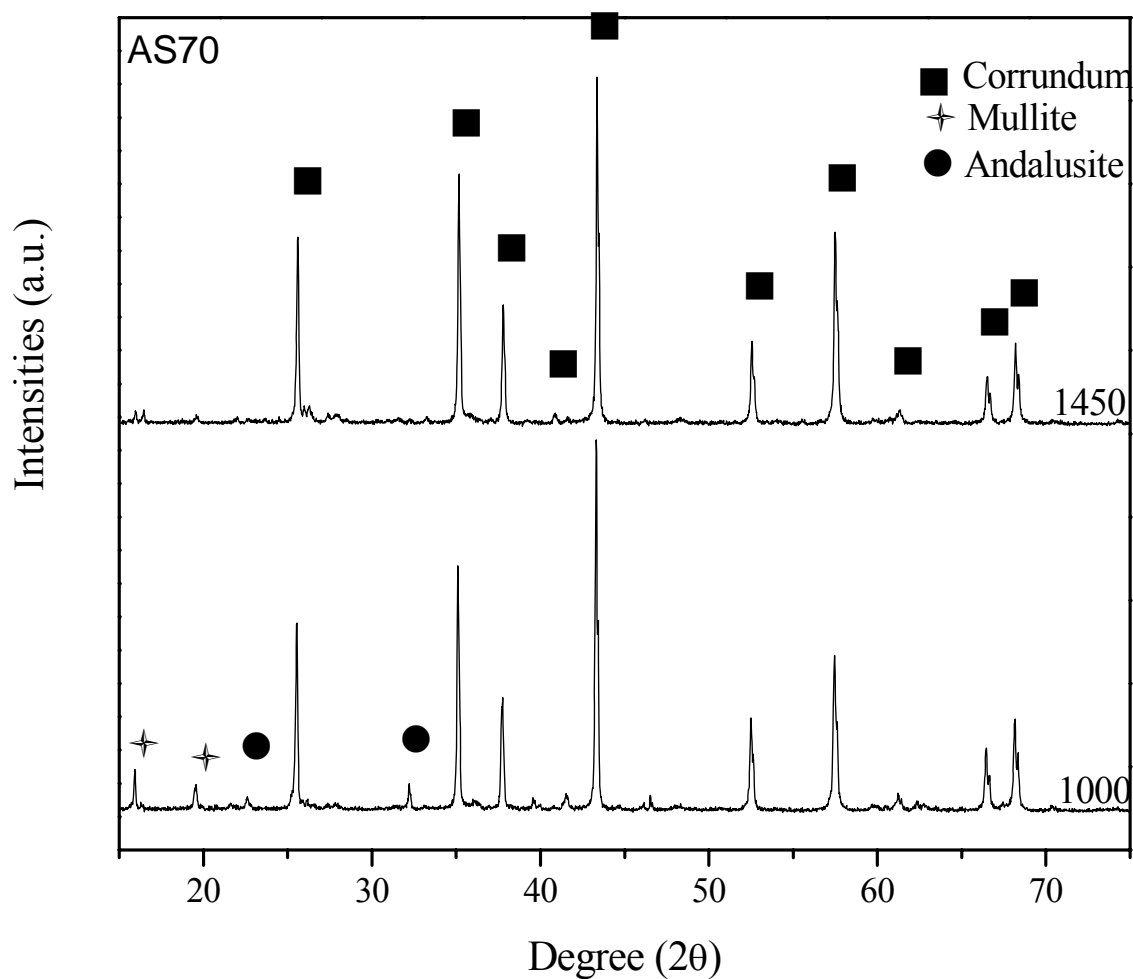


Fig. 4.9 XRD pattern of the fired AS70 composition

Table 4.7 – Semi quantitative analysis of 1450°C fired castables

composition	A	AS70	AS80
Alumina	76	80	68
Mullite	13	9	10
Andalusite	11	6	10
Anorthite	Trace	6	12

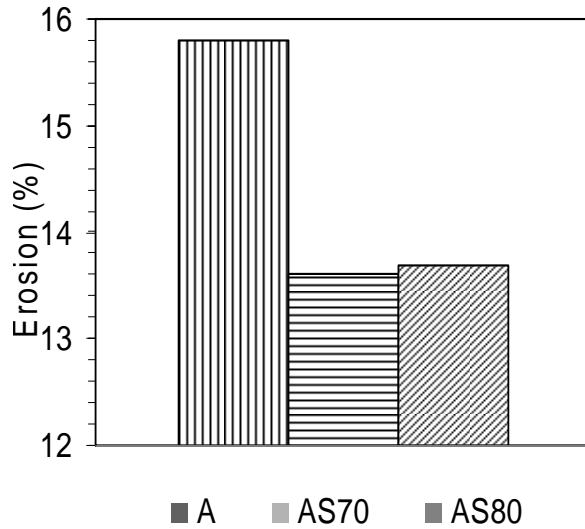


Fig. 4.10 Erosion behavior of Castable group-A



Fig. 4.11. Photograph of eroded samples

4.5 Characterization of Castable Group-B

4.5.1 Sieve Analysis of dry mix

The sieve analysis of Castable group-B is shown in Fig.4.12. It has been observed that the fine fraction of particles having size less than 45 μ m content in all categories is greater than 30% which come under suitable range. The fine fraction in BS80 is more but the coarse particles are found to be maximum in B type composition. The particle size distribution in the BS80 composition approaches the region of good strength as described in the literature [24].

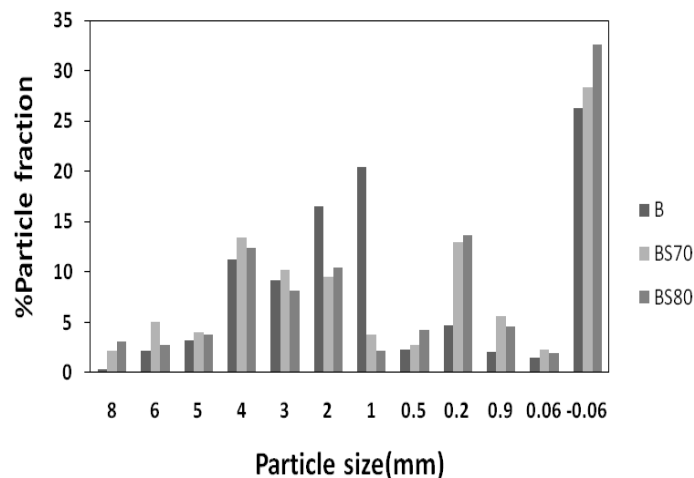


Fig. 4.12 Sieve Analysis of Castable group-B

4.5.2 Chemical Analysis

The chemical analysis result of Castable group-B is listed in the table-4.8. The result shows that this group of castables contains more than 80% Al_2O_3 . The iron oxide and titania content in all the compositions are approximately 1%. The lime contain in the indigenous cements are relatively more.

Table 4.8 Chemical Compositions of the Castable group-B

Chemical Component (wt%)	Castable group B		
	B	BS70	BS80
Al_2O_3	83.87	80.49	83.03
Fe_2O_3	0.70	0.84	0.88
TiO_2	0.8	1.0	1.1
CaO	0.70	1.11	0.9

4.5.3 Physical properties

The physical properties of Castable group-B are listed in Table 4.9. It is clearly observed that the water demand for casting BS70 is relatively more than the other two compositions. Even if the water of casting is more it did not have good flow. This has higher setting time. This abnormality is believed to be due to the material defect and experimental casting parameters. It was observed during casting of this material that the material seems to be very thirsty and the water added was quickly absorbed continuing the dryness of the material. The visual inspection showed that the nonpliability of the material enhances the dilatancy. So for its casting in the mold more vibration had to be given. This undesirable behaviour affects severely the rheological behavior of the castable. The water requirement, flow behavior and the setting time of B and BS80 compositions are in the desirable range. The relatively higher setting time of the composition BS70 and BS80 are attributed to their fineness.

The graphical representation of the variation of the apparent porosity and bulk density of the different composition of Castable group-B with temperature are shown in (Fig-4.13) and (Fig-4.14). It is found that the apparent porosity in BS70 (10.6%) is higher than the other two compositions B (9.9%) and BS80 (7.9%) because of higher water demand and less packing due to low flowability. The bulk density was found accordingly. The porous material posses lower density and vice versa. It has been observed that the apparent porosity in B and BS80

increases gradually but the trend is slightly different in case of BS70. The decrease in apparent porosity trend from 1000°C onward is attributed to the more formation of liquid phase which entrapped the pores providing denser structure. This is due to the higher content of lime in the cement used in BS70.

Table 4.9 Physical Properties of Castable group-B

Physical Properties	Castable group-B		
	B	BS70	BS80
Water of casting (wt. %)	4.40	5.20	4.10
Vibro-flow(mm)	200	180	200
Initial Setting time(minute)	55'	120'	110'
Apparent Porosity 110° C/24hrs	9.9	10.6	7.9
1000° C/3hrs	13.4	15.0	11.6
1450° C/3hrs	15.6	12.2	12.9
Bulk Density(gm/cc) 110° C/3hrs	3.07	3.01	3.12
1000° C/3hrs	3.02	2.95	3.11
1450° C/3hrs	3.00	3.04	3.09

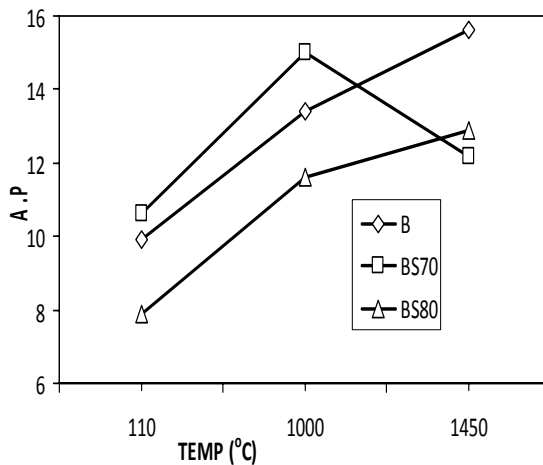


Fig. 4.13 Variation in AP with temperature

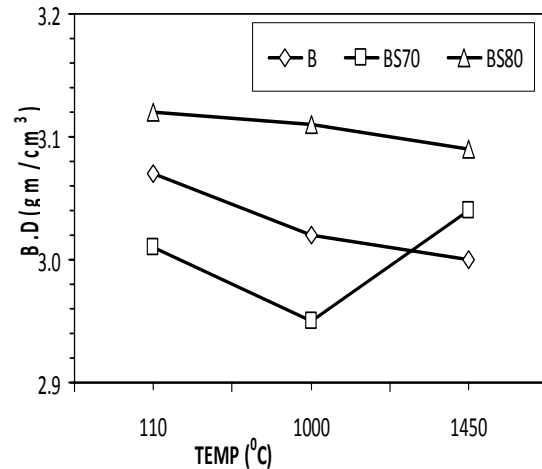


Fig. 4.14 Variation in BD with temperature

4.5.4 Mechanical properties

The result of mechanical properties found in the Castable group-B is summarized in Table-4.10. The schematic diagrams of variation of CCS and CMOR with temperature are given in Fig-4.15 and Fig-4.16. The difference in drying strength observed is due to the difference in

the mineralogical phases present in different cements. There is a drastic change in high temperature CCS of the BS80 composition. This behaviour may be due to the lower amounts of casting water and having a good rheological property. There is a good flow which provides better moulding compactness. Also it has been observed that the particle size distribution in the BS80 falls in the high strength region of schematic particle size diagram for castable which provides better strength [4]. Accordingly the cold moduli of rupture are found superior.

As the cement used in BS70 contain more amount of lime, due to its fluxing nature it produces more liquid phase by reacting with impurities like Fe_2O_3 and TiO_2 at 1000°C . It also formed glassy phases like gehlinitite (C_2AS) and anorthite (CAS_2) phases at temperature more than 1400°C . So the PLCs in BS70 came negative. The hot modulus of rupture of BS70 is found to be low. This is due to the high lime content in the cement used in this composition. This is the reason why the CMOR of BS70 comes lower at 1450°C .

Table 4.10 Mechanical Properties of Castable group-B

Physical Properties	Castable group-B		
	B	BS70	BS80
CCS(kg/cm^2) 110 ⁰ C/24hrs	338	513	250
1000 ⁰ C/ 3hrs	581	525	1325
1450 ⁰ C/ 3hrs	912	725	1356
CMOR(kg/cm^2) 110 ⁰ C /3hrs	76	91	76
1000 ⁰ C/3hrs	152	152	198
1450 ⁰ C/3hrs	152	137	168
HMOR(kg/cm^2) 1400 ⁰ C/30min	17	8	12
PLC(%) 1000 ⁰ C/3hrs	+0.03	-0.12	-0.07
1450 ⁰ C/3hrs	+0.41	-0.39	+0.09
EROSION (%)	13.21	15.42	7.16

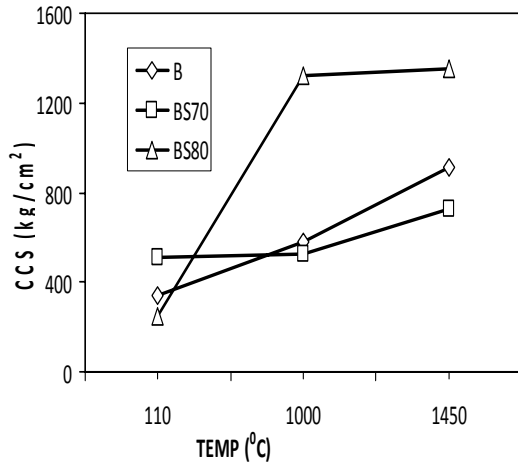


Fig.4.15 Variation in CCS with temperature

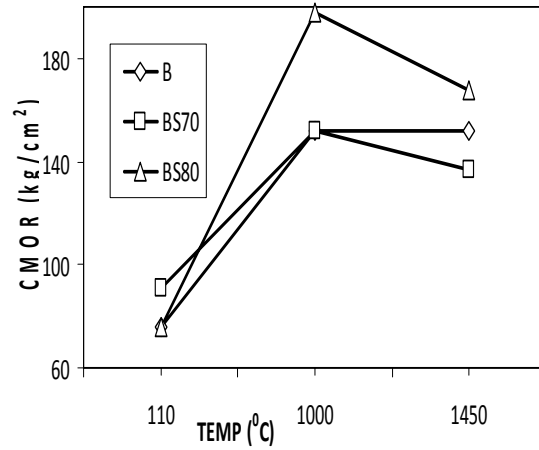


Fig.4.16 Variation in CMOR with temperature

The erosion behavior of the castable group-B is shown in Fig.4.17. The photo graph of the eroded sample after demoulding from rotary drum is shown in Fig.4.18. The erosion resistances of this group of castables are found to be superior because of higher percent of WFA (57%) and Densd bauxite (32.5%) used in the compositions. These materials provide mores densed structure to the castables due to their densed nonporous grains.

The castable BS80 was not corroded more. This is due to the fact that it possess very low porosity, well particle packing and having highly densed structure at all the stages of firing. It was also observed that there is a positive PLC found at higher temperature which makes the structure more toughen by arresting any crack propagation. Due to the densed microstructure it does not allow the infiltration of molten metal and slag into the bulk of the material. The castable BS70 is comparatively more corroded because of its relatively porous microstructure.

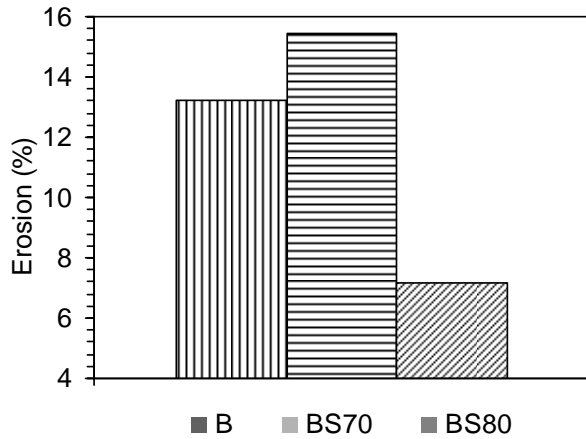


Fig. 4.17 Erosion behaviour of Castable group-B



Fig. 4.18 Photograph of eroded samples

4.6 Characterization of Castable Group-C

4.6.1 Sieve Analysis of dry mix

The sieve analysis showing the particle size distribution of the castable group-C is shown in Fig-4.19. The fine fraction content in all the compositions is ~30%. The medium size particle fraction in composition-C is ~18% where as its content in CS70 and CS80 are ~10%. The coarse fraction varies according to the variation in the medium size particle fraction because the fine fractions are almost same in all the compositions.

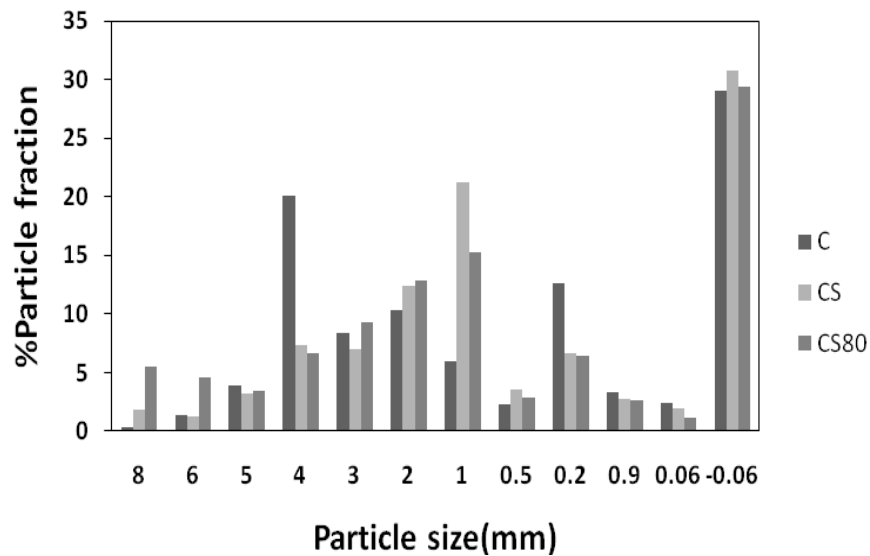


Fig. 4.19 Sieve Analysis of Castable group-C

4.6.2 Chemical Analysis

The chemical analysis of the different subgroup of castable group C is given in the Table-4.11. It has been seen that the alumina content in the compositions are not so high. It is ~60%. The lower alumina content is due to presence of the relatively lower alumina based material like calcined clay (~38% Al_2O_3) and densed bauxite (90% Al_2O_3) as compared to the WFA, BFA ad calcined alumina. The lime content in the CS70 and CS80 are much higher. The higher percentage of the Fe_2O_3 and TiO_2 are due to the use of 71% densed bauxite in the composition which content significant amount of these impurities phases.

Table 4.11 Chemical Compositions of the Castable group-C

Chemical Component (wt.%)	Castable group-C		
	C	CS70	CS80
Al_2O_3	61.2	58.81	60.13
Fe_2O_3	0.82	0.78	0.84
TiO_2	1.34	1.48	1.19
CaO	0.85	1.60	1.45

4.6.3 Physical Properties

All the composition of this group of castable needs almost equal amount of water to achieve the required rheological behavior. Accordingly the flow behaviors are also similar. The setting time of C and CS70 are in the workable range but the setting time of CS80 is relatively short.

The apparent porosity of C is much higher than the other two compositions (Table 4.12). The relative lower BD in the all the compositions are due to the use of porous aluminum silicate materials like the calcined clays as shown in Fig. 4.20 and Fig. 4.21 respectively. The generation of higher porosity at the intermediate temperature is attributed to the removal of chemically bonded waters and also the formation of micro porous zeolitic phases. The observed reduction in porosity above 1000°C is due to the formation of ceramic bond by sintering.

Table 4.12 Physical Properties Castable group-C

Physical Properties	Castable group-C		
	C	CS70	CS80
Casting water (%)	4.20	4.33	4.21
Vibro-flow(mm)	190	190	180
Initial Setting time(minute)	55'	60'	45'
Apparent Porosity 110° C/24hrs	9.4	8.57	8.3
1000° C/3hrs	13.9	12.2	12.7
1450° C/3hrs	14.2	11.9	12.4
Bulk Density(gm/cc) 110° C/3hrs	2.65	2.70	2.70
1000° C/3hrs	2.61	2.67	2.67
1450° C/3hrs	2.56	2.64	2.64

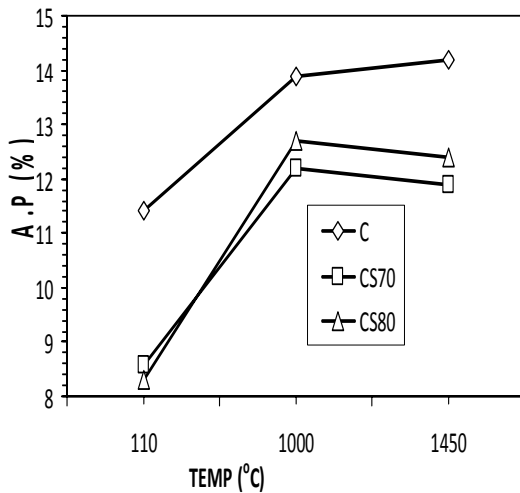


Fig. 4.20 Variation in A.P with temperature

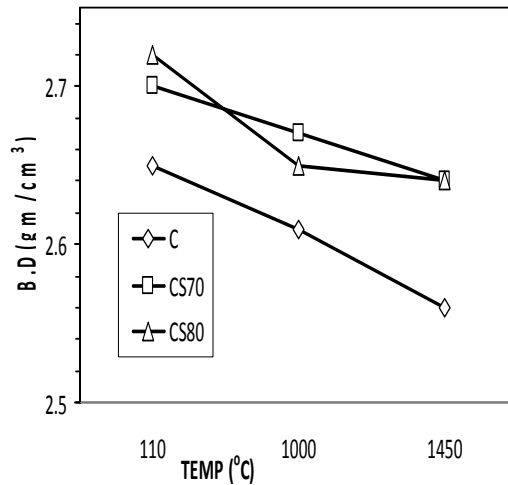


Fig. 4.21 Variation in B.D with temperature

4.6.4 Mechanical Properties

Fig. 4.22 shows the CCS of Castable group-C. The higher CCS of CS70 is due to the higher amount of CA phase in the cement. The cold crushing strength of the composition C is relatively low because due to low apparent porosity (Table 4.13). The cold crushing strength of CS80 is superior due to enhanced mullitization (~40%) as observed from XRD analysis.

The CMOR value of the CS70 composition is superior as compared to the other two compositions although it contains relative low amount of alumina and higher percentage of lime (Fig. 4.23). This may be due to observed higher strength as discussed above.

The positive PLCs in all the cases are due to the presence of calcined clay in these castable compositions which undergoes volume expansion due to mullitization at higher temperature. The positive effect on strength of alumina–silicate may be caused by a combination of two mechanisms. First, the transformation which may begin below 1300°C in the presence of impurities, acts as a seed for further mullite formation [50,51]. Second, the volume increase of andalusite and kyanite occurring in the liquid phase will force the liquid to fill the pores. This movement of liquid phase may also be beneficial to the solution/precipitation process from which mullite is supposed to develop.

Table 4.13 Mechanical Properties of Castable group-C

Mechanical Properties		Castable group-C		
		C	CS70	CS80
CCS(kg/cm ²)	110°C/24hrs	238	400	337
	1000°C/3hrs	545	656	925
	1450°C/3hrs	575	531	906
CMOR(kg/cm ²)	110°C /24hrs	91	76	91
	1000°C/3hrs	76	106	69
	1450°C/3hrs	91	122	84
HMOR(kg/cm ²)	1400°C/30min	10	18	9
PLC(%)	1000°C/3hrs	+0.36	+0.27	+0.25
	1450°C/3hrs	+1.15	+0.83	+0.59
EROSION (%)		29.24	28.54	27.8

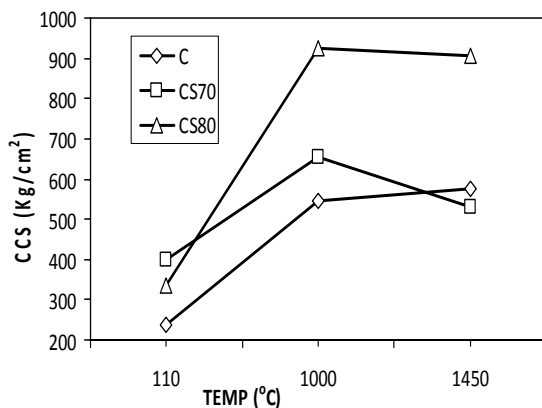


Fig. 4.22. Variation in CCS with temperature

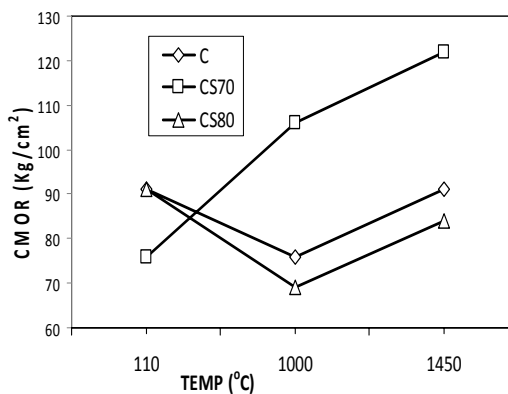


Fig. 4.23. Variation in CMOR with temperature

The erosion behavior of the Castable group-C is shown in Fig. 4.24. The photograph of the eroded sample after demoulding from rotary drum is shown in Fig. 4.25. The castables CS70 and CS80 show better resistance to erosion. This is directly related to the fact that they possess very low porosity, well particle packing and having highly dense structure at all the stages of firing. It was also observed that there is a positive PLC found at higher temperature in all the compositions which makes the structure more toughen by arresting any crack propagation. Due to the dense microstructure it does not allow the infiltration of molten metal and slag into the bulk of the material.

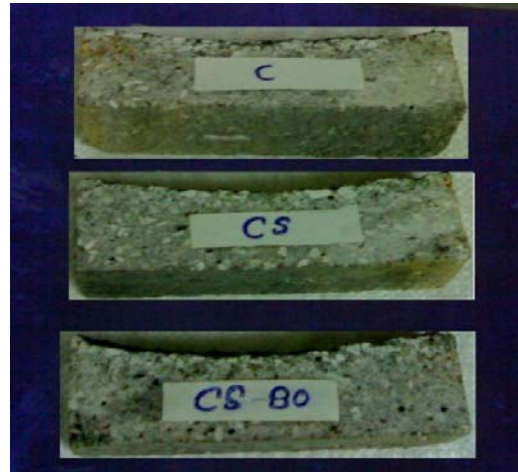
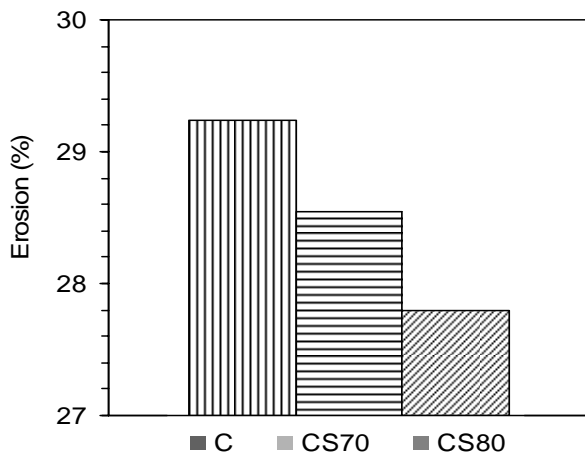


Fig. 4.24. Erosion behaviour of Castable group-C

Fig. 4.25. Photograph of eroded samples

4.7 Characterization of Castable Group-D

4.7.1 Sieve Analysis of dry mix

The particle size distribution of the castable group-D is shown Fig-4.26. shows its corresponding graphical representation. The fine fraction content in all the compositions is ~30%. The medium size particle fraction in composition-D is 24% where as its content in DS70 and DS80 are ~20%.

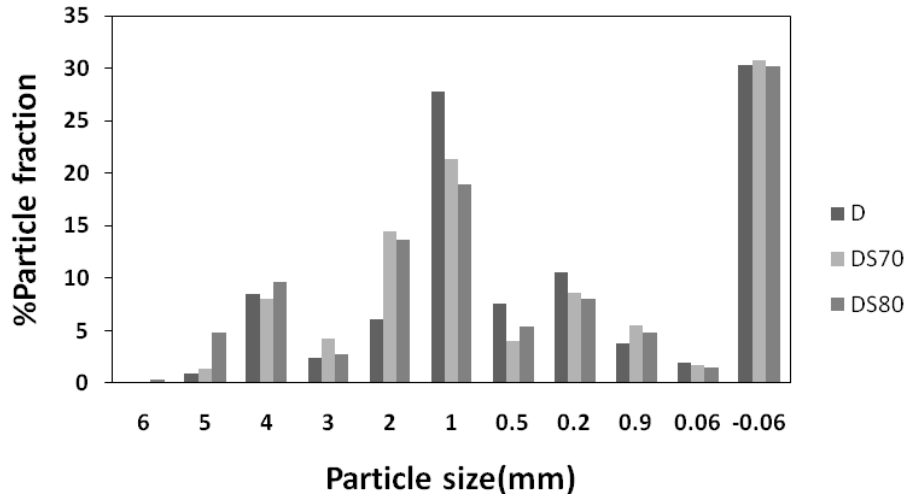


Fig. 4.26. Sieve Analysis Castable group-D

4.7.2 Chemical Analysis

The chemical analysis of the different subgroup of Castable group-D is given in the Table 4.14. It has been seen that the alumina content in the compositions ~80%. The lime content in the DS70 and DS80 are comparatively higher than D composition. The iron oxide and titania content of the D composition is comparatively higher than the other two compositions.

Table 4.14 Chemical Compositions of the Castable group-D

Chemical Component(wt%)	Castable Group-D		
	D	DS70	DS80
Al ₂ O ₃	79.48	80.42	79.68
Fe ₂ O ₃	1.40	0.72	0.76
TiO ₂	1.44	1.10	0.62
CaO	0.92	1.56	1.43

4.7.3 Physical Properties

The physical properties of the Castable group-D are listed in the Table 4.15. The different composition of this group of castable requires different amount of water to achieve the required rheological behavior. The flow behaviors are almost similar although a significant difference in the water of casting.

A sudden degradation in the flow was observed. This behavior is not solely dependent on the type of cement used but the material quality has a significant effect on it. The setting time of

D and DS70 are in the workable range but the setting time of DS80 is relatively short even if the water requirement in this composition is more. The apparent porosities are found according to the water demand for casting in all compositions. The bulk density came accordingly (Fig. 4.27 & 4.28).

Table 4.15 Physical Properties of Castable group-D

Physical Properties	Castable group-D		
	D	DS70	DS80
Casting water (%)	4.90	5.26	6.05
Vibro-flow(mm)	180	180	180
Initial Setting time(minute)	70'	65'	40'
Apparent Porosity 110 ⁰ C/24hrs	13.0	13.2	14.0
1000 ⁰ C/3hrs	16.1	18.4	18.4
1450 ⁰ C/3hrs	16.9	18.3	17.9
Bulk Density(gm/cc) 110 ⁰ C/3hrs	2.78	2.81	2.82
1000 ⁰ C/3hrs	2.73	2.82	2.79
1450 ⁰ C/3hrs	2.72	2.79	2.81

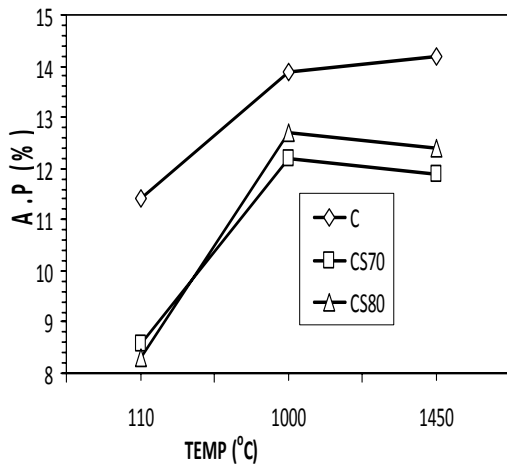


Fig. 4.27 Variation in A.P. with temperature

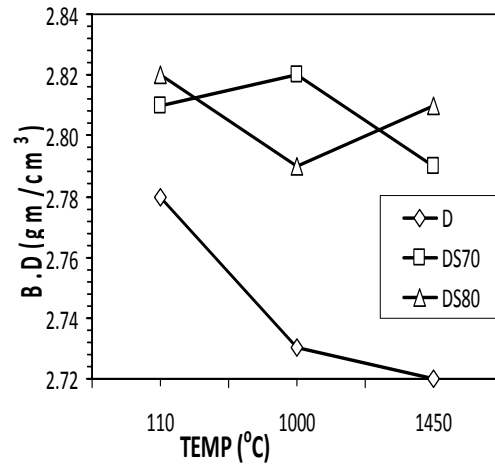


Fig. 4.28 Variation in B.D. with temperature

4.7.4 Mechanical Properties

The cold crushing strengths in all the compositions are low (Fig. 4.29). It has a direct relationship with the type of cement used, the water of casting and the curing temperature. The lower cold crushing strength of DS80 is due to the higher water of casting which generated a lot of porosity in the structure decreasing the strength at all stages of firing.

The HMOR values of all the compositions are found to be very low (Fig. 4.30). This may be due to the higher percentage of lime (Table 4.16). The PLCs in all the cases are positive due to the presence of calcined clay in these castable compositions which undergoes volume expansion due to mullitization at higher temperature [51].

Fig.4.31 shows the erosion behavior of the castable group-D. The photo graph of the eroded sample after demoulding from rotary drum is shown in Fig. 4.32. The all castables shows very less resistance to erosion. This is directly related to porosity, bulk density, percentage mullite formation as well the glassy phase formation. The more porous structure at high temperature allow the infiltration of molten metal and slag into the bulk of the material and eroded more due to peeling.

Table 4.16. Mechanical Properties of Castable group-D

Mechanical Properties		Castable group-D		
		D	DS	DS80
CCS(kg/cm ²)	110°C/24hrs	263	138	125
	1000°C/3hrs	781	406	238
	1450°C/3hrs	662	513	531
CMOR(kg/cm ²)	110°C/24hrs	91	46	46
	1000°C/3hrs	91	152	69
	1450°C/3hrs	106	198	168
HMOR(kg/cm ²)	1400°C/30min	10	7	9
PLC(%)	1000°C/3hrs	+0.06	-0.40	+0.01
	1450°C/3hrs	+0.49	+0.30	+0.09
EROSION (%)		31.29	18.98	23.86

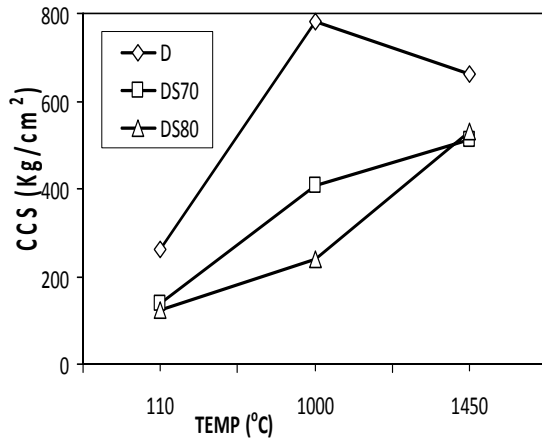


Fig. 4.29 Variation in CCS with temprature

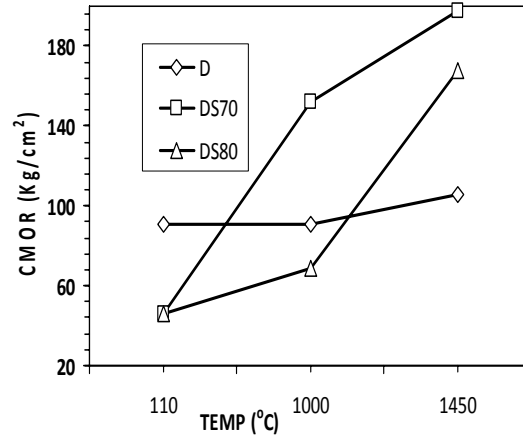


Fig. 4.30 Variation in CMOR with temprature

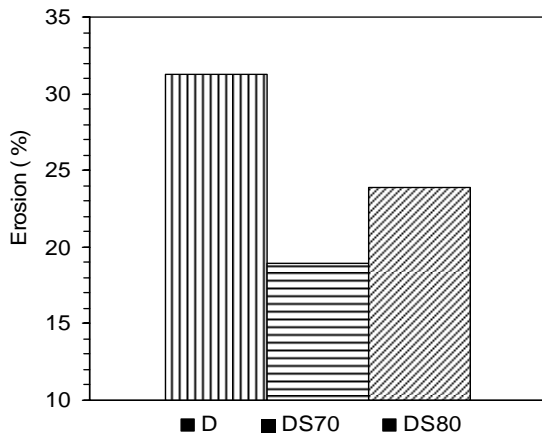


Fig. 4.31 Erosion behaviour of Castable group-D

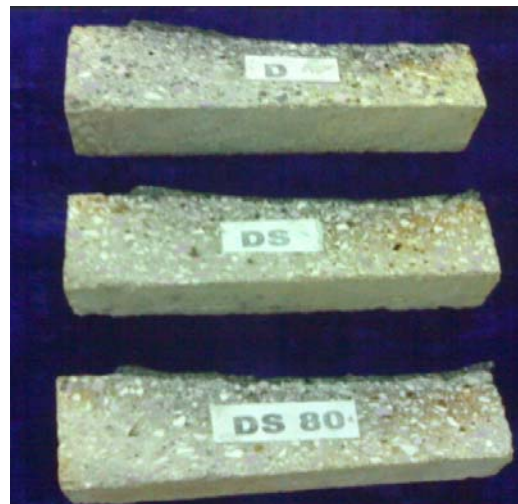


Fig. 4.32 Photograph of eroded samples

4.8 Comparison between the Erosion behaviors of different group of castables

4.8.1 Castables with imported cement (CA-25)

The erosion behaviors of different groups of castables with imported cement are shown in the Fig. 4.33. It has been seen that samples A and B have more resistance to erosion as compared to the samples C and D. The erosion percentage of castable D is highest among all as the apparent porosity of 1450°C fired D sample is highest (16.9%). Due to higher porosity, easy infiltration of the molten metal and slags to the bulk of the material happens. It has also been

observed that the combination of aggregate materials used in the samples have a direct relationship with the slag erosion. The materials contain higher percentage of WFA and BFA are less prone to corrosion because of their chemical inertness, densed grain and lower impurities content. Among these four type of aggregate combination, composition B is best suited for imported cement.

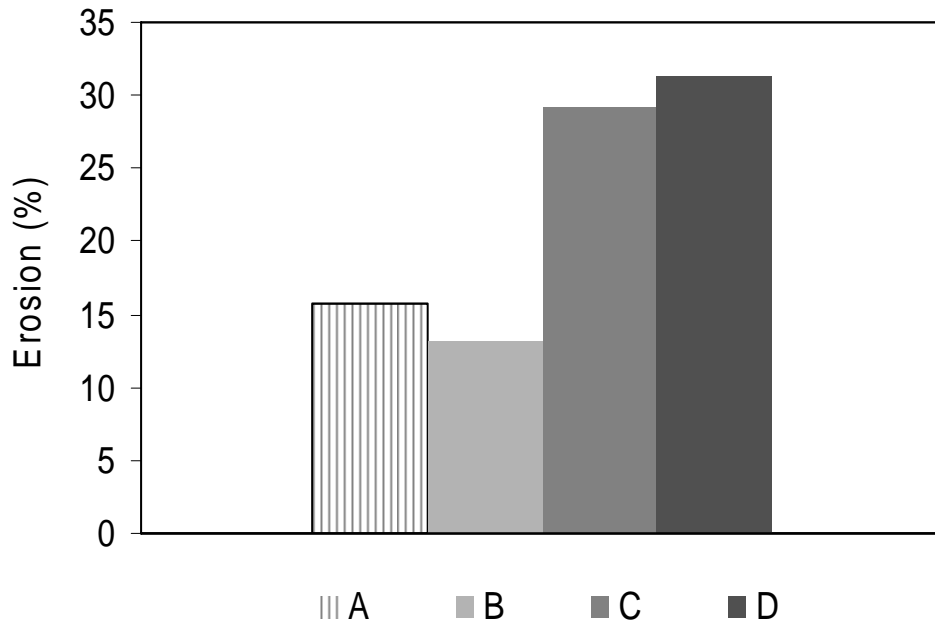


Fig. 4.33 Erosion behaviour of different group of castables with CA-25 cement

4.8.2 Castables with indigenous cements

The erosion behaviors of different groups of castables with indigenous cements HAC-70 and HAC-80 are shown in the Fig.4.34 and Fig.4.35 respectively. It has been observed WFA and BFA aggregate plays important role on the erosion resistance. It has been found that aggregate composition A is best suited for 70%Al₂O₃ containing indigenous cement. However composition B is the best for 80% containing indigenous cement.

Among all the aggregate composition and cement combination studied, composition B i.e. (Calcined Alumina ~5%, WFA ~57.5%, Densd Bauxite ~32.5%, Microsilica ~4%, CAC ~2%, Aluminum powder ~0.4%, SHMP ~0.05%, Ammonium borate ~0.02%) with 70%Al₂O₃ containing indigenous cement shows best erosion resistivity i.e. 7.16%.

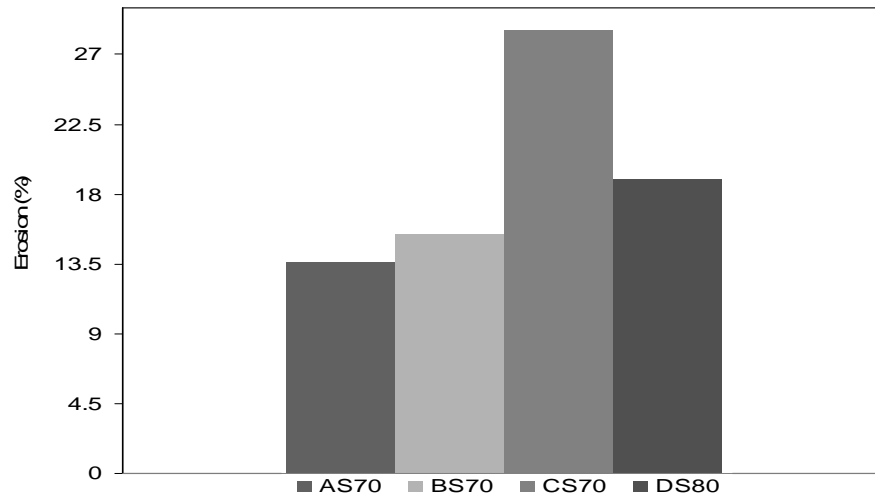


Fig. 4.34-Erosion behaviour of different group of castables with HAC-70 cement

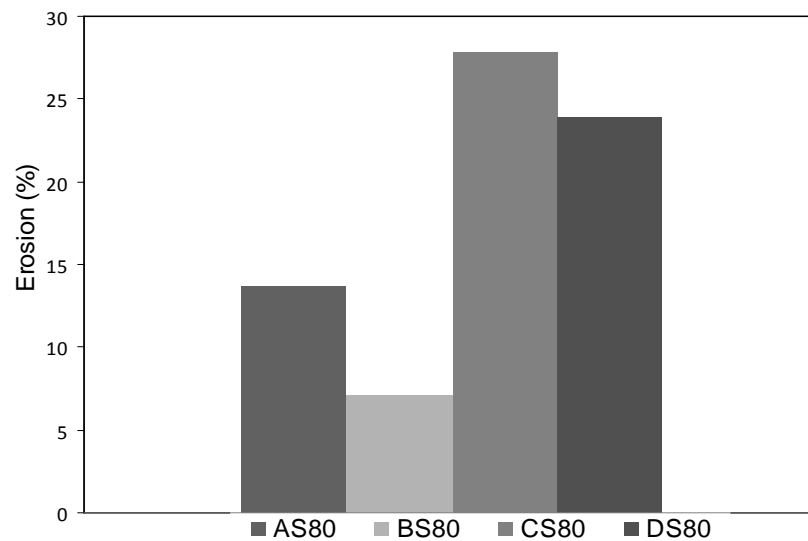


Fig. 4.35 Erosion behaviour of different group of castables with HAC-80 cement

Finally it can be concluded that the indigenous cement can replace imported cement to manufacture an industrial ULCC for 1600°C slag corrosion zone application. It has been found that the same parameters like purities and chemical inertness of materials used, apparent porosity, bulk density and the strength of the casted samples has direct relationship with the observed erosion resistance of the different group of castables with indigenous cements.

Chapter-5

Conclusion

5.0 Conclusions

1. ULCC composition having higher amount of BFA aggregate shows better slag corrosion resistance when indigenous HAC are used.
2. However ULCC containing WFA shows better slag resistance when 80% Al_2O_3 containing indigenous cement were used.
3. It was found that slag resistivity mainly depend on fused alumina aggregate content of ULCC. The composition without having BFA and WFA shows very high (about 28%) erosion.
4. Fused alumina aggregates show better erosion resistance than Densed Bauxite.
5. Slag erosion resistivity of Densed Bauxite based ULCC increased upon WFA addition.
6. 70% Al_2O_3 containing indigenous cement shows better erosion resistivity performance in presence of BFA.
7. However 80% Al_2O_3 containing indigenous cement shows better performance in presence of WFA.

References

- [1] Iron and steel review Vol-50, No-07, Dec-2006
- [2] B. V. Raja, P.sahu , J.d panda “Status & Outlook of Indian Refractory Industry”, steel world, June -2006(9-13)
- [3] S N Laha, “Non Recovery Coke Ovens - An Overview & An Innovative Indian Refractories Experience”, VOL. 9, NO. 1 February 2006, IIM Metal news
- [4] K. Sugita, “Status of Refractories and Steel Technology in Japan: Progress during the Past Half Century”, UNITECR’ 95 (Kyoto, Japan, 1995), 103-132.
- [5] Y. Shinohara, H. Yaoi, and K. Sugita, “Recent Progress in Monolithic Refractories Usage in the Japanese Steel Industry”, New Developments in Monolithic Refractories in Advances in Ceramics 13 1-20 (1984)
- [6] W.E. Lee, W. Viera, S. Zang, K. Ghanbari Ahai, H. Sarpoolaky, C.Parr, “Castable Refractory Concrete”, Int. Mater. Rev. 46 (3) (2001) 145–167
- [7] L. P. Krietz, “Monolithic and Fibrous Refractories”, pp. 910-917 in Engineered Materials Handbook Vol. 4 Ceramics and Glasses (ASM Int’l., 1991)
- [8] T. Eguchi, I. Takita, J. Yoshitomi, S. Kiritani, and M. Sato, “Low-Cement-Bonded Castable Refractories”, Taikabutsu Overseas 9 [1],(1989), 10-25
- [9] H. Nakashima, S. Sudo, I. Takahashi, and E. Konishi, “Application of Self-Flow Type Castable Refractories in NKK”, Proc. UNITECR’ 95 (Kyoto, Japan, 1995), 205-213.
- [10] A. Watanabe, H. takahashi, S. Takanaga, and M. Uchida, “Magnesia Containing Basic Castables”,Proc. UNITECR’ 95 (Kyoto, Japan, 1995), 181-188.
- [11] J. Yamada, S. Sakaki, K. Kasai, H. Ishimatsu. “Application technology of monolithic refractories in NSC, in: Proceedings of the Unified Int. Tech. Conf. on ‘Refractories’ (UNITECR ‘95), Kyoto, Japan, 1995, pp. 277–84.
- [12] A. Nishikawa, “Technology of Monolithic Refractories”, Plibrico Japan Co. Ltd., Tokyo, Japan, 1984.
- [13] L. P. Krietz, R. E. Fisher, and J. G. Beetz, “Evolution and Status of Refractory Castable Technology Entering the 1990s”, Am. Ceram. Soc. Bull. 69 (1990), 1690-93
- [14] G. MacZura, L. D. Hart, R. P. Heilich, and J. E. Kopanda, “Refractory Cements”, Ceram.Sci. Eng. Proc., 4 [1-2], (1983), 46-65

- [15] J. E. Kopanda and G. MacZura, "Production Processes, Properties, and Applications for Calcium Aluminate Cements" in Alumina Chemicals - Science and Technology Handbook, 171-183, Am.Ceram. Soc., Westerville, Ohio, 1990.
- [16] C. Richmond and C. E. Chaille, "High-Performance Castables for Severe Applications", New Developments in Monolithic Refractories in Advances in Ceramics 13(1984), 230-244
- [17] S. Banerjee, R. V. Kilgore, and D. A. Knowlton, "Low-Moisture Castables: Properties and Applications", New Developments in Monolithic Refractories in Advances in Ceramics 13(1984), 257-273
- [18] Refractories production and properties, J.H Chesters, The iron and steel institute, London, Carlton house Terrace, p.99- 100
- [19] W. Krönert, "Recent Progress in the Use of Monolithic Refractories in Europe", New Developments in Monolithic Refractories in Advances in Ceramics 13 (1984). 21-45
- [20] G. MacZura, "Production Processes, Properties, and Applications for Tabular Alumina Refractory Aggregates", in Alumina Chemicals-Science and Technology Handbook, 109-170, The Am. Ceram. Soc. Inc., Westerville, Ohio, 1990.
- [21] B. Myhre, "The Effect of Particle Size Distribution on Flow of Refractory Castables", presented at The American Ceramic Society 30th Annual Refractory Symposium in St. Louis, Missouri, March 25, 1994.
- [22] B. Myhre and K. Sunde, "Tabular Alumina Based Refractory Castables - Part 1: The Effect of Microsilica Additions on Flow and Cold Strength of Tabular Alumina Based Low and Ultralow Cement Castables", Technical Report (Elkem).
- [23] Mr B. N. Ghose, "Corrosion of refractories—an outline "Workshop on Corrosion of Refractories in Iron and Steel making, Organized by the Indian ceramic society, Jamshedpur chapter
- [24] Hamed Samadi, "The effect of particle size distribution on physical properties of castables" PARS Refractories Co., Tehran, IRAN
- [25] Rafael G. Pileggi, André R. Studart, Victor C. Pandolfelli "Mixing and rheology of refractory castables"UNITECR 2001,1357-1372
- [26] Fabio A.Cardoso, Murilo D.M. Innocentini, Mario M. Akiyoshi, Victor C. Pandolfelli, "Effect of curing time on the properties of CAC bonded refractory castables".
- [27] M. R. Nilforoushan, M. R. Saerie, S. Otraj "Phase formations and their effects on properties of a refractory calcium aluminate cement",UNITER-05

- [28] C. Alt, L. Wong, C. Parr, Measuring castable rheology by exothermic profile, *Refractories Applications and News* 8 (2) (2003) 15–18.
- [29] C.M.George, “Aspects of calcium aluminate cement hydration, in: *Refractories Symposium*, The American Ceramic Society, St. Louis, 1994 , pp. 1–21.
- [30] J.M. Rivas Mercury, X. Turrillas, A.H. de Azaa, P. Pena “Calcium aluminates hydration in presence of amorphous SiO₂ at temperatures below 90 °C”, *Journal of Solid State Chemistry*.
- [31] I.R. Oliveira , F.S. Ortega , V.C. Pandolfelli “Hydration of CAC cement in a castable refractory matrix containing processing additives”, *CERAMIC INTERNATIONAL*
- [32] S.A. Rodger and D.D. Double, “The chemistry of Hydration of High Alumina Cement in the presence of Accelerating and Retarding admixtures”, *CEMENT and CONCRETE RESEARCH*. Vol. 14, pp. 73-82, 1984.
- [33] Thomas A. Bier, Alain Mathieu, Bruno Espiosa, Christophe Marcelon “Admixture and their interactions with high range calcium aluminate cement”. *Iron & Steel Review*, August 2008
- [34] N. Bunt, C. Revais, M. Vialle, Additives in calcium aluminates cement containing castables, in *Proceedings of UNITECR 97* vol. III, pp. 1347–1354.
- [35] I.R. Oliveira, V.C. Pandolfelli “Castable matrix, additives and their role on hydraulic binder hydration”, *Ceramics International* 35 (2009), 1453–1460
- [36] Benoit Valdevier, Christoph Wohrmeyer, Christopher Parr “Application of calcium aluminate cement to dense low water demand refractory castable” *IREFCON 2002*
- [37] V.K. Tiwary, I.N. Chakraborty, A study on Hydration of Calcium Aluminate Cement (CAC) phases with Siliceous Material, *IREFCON-2008*, 193-198
- [38] H.Peng, B.Myhre, J.Li, S.Tian, F.Gan “Effect of Microsilica on Properties of Corundum-Mullite Self-Flow ultra- Low cement Castable” *IREFCON 2008*, 177-183.
- [39] S. Maitra, S. Bose, N. Bandyopadhyay, A. Roychoudhury, “Dehydration kinetics of calcium aluminate cement hydrate under non-isothermal conditions”, *Ceramics International* 31 (2005), 371–374
- [40] Jian Ding, Yan Fu and J.J. Beaudoin, “Effect of Different Inorganic Salts/Alkali on Conversion-Prevention in High Alumina Cement Products”. *ELSEVIER*
- [41] M.T. Gaztafiaga, S. Gofii 1 and J.L. Sagrera, “Reactivity of high-alumina cement in water: pore-solution and solid phase characterization”, *Solid State Ionics* 63-65 (1993), 797-802

- [42] Karen L. Scrivener, Jean-Louis Cabiron, Roger Letourneux, "High-performance concretes from calcium aluminate cements, Cement and Concrete Research 29 (1999), 1215–1223
- [43] K. Sankaranarayanan, P. Singh, "Correlation between flow, flow decay and salient parameter of alumina based self-flow castable" IRFCOON 2002/II, 41-47
- [44] Moreno.R "The role of slip additives in the tape casting technology". Part-I Solvent and dispersons", Am.Cer.Soc.Bull.
- [45] Z.Li, S.Zhang, N.Zhou and G.Ye "Difference in dispersing effect between organic and inorganic deflocculants in castable" Proceedings of UNITECR'97, 3(1997),1355-1361
- [46] Zhanmin Wang, Xiyang Cao, Qiang Wang "Effect of aluminium addition on properties of Al_2O_3 -SiC-C dry ramming mixes for BF trough", UNITECR07
- [47] Subrata Barua "Introduction to Monolithic Refractory"
- [48] A.R. Studart, M.D.M. Innocentini, I.R. Oliveira, V.C. Pandolfelli "Reaction of aluminum powder with water in cement-containing refractory castables" Journal of the European Ceramic Society 25 (2005), 3135–3143
- [49] Pavlo Kryvoruchko, Yuliya Mishnyova, Nina Girich, Olena Sinyukova, Natalia Pryvalova "Properties dependence of alumina refractories on the kind of the used alumina – either sintered or fused", UNITECR07
- [50] P.Prigent, Dr P.Hubert, Damrec, Mine de Glomel, Pr M.Rigaud, "Behaviour of Andalusite in the matrix of High Alumina Low Cement Castables", UNITECR-05
- [51] V. Viswabaskaran, F.D. Gnanam, M. Balasubramanian, "Mullitisation behaviour of calcined clay–alumina mixtures", Ceramics International 29 (2003), 561–571
- [52] M.F.M. Zawrah, N.M. Khalil "Effect of mullite formation on properties of refractory castables" Ceramics International 27 (2001), 689–694
- [53] H. Sarpoolaky1, K.G. Ahari, W.E. Lee "Influence of in situ phase formation on microstructural evolution and properties of castable refractories", Ceramics International 28 (2002), 487–493